MODELING OF FERRITE CONTENT IN THE SIMULATED HEAT AFFECTED ZONE (HAZ) OF DUPLEX STAINLESS STEEL

Júlia de Oliveira Noldin

ENSIACET Tutor: Julitte HUEZ

Aperam Tutor: Jérôme BRIDEL

September 2024

Acknowledgement

I would like to express special thanks to:

My tutors at Aperam Isbergues M. Jérôme BRIDEL and M. Bertrand PETIT, for having welcomed and guided me during this period; Prof. Julitte HUEZ, my tutor at ENSIACET.

The International Relations Office of ENSIACET, for the assistance with all the bureaucratic procedures to make this a reality.

The coordination of undergraduate studies in Materials Engineering at the Federal University of Santa Catarina (UFSC), my institution of origin in Brazil, and Prof. Guilherme Barra for the support throughout the BRAFITEC program along with CAPES;

To all my friends and co-workers, for the competence in passing the knowledge and technical instructions on laboratory instrumentation.

My family, especially my mom, dad and my two sisters who always supported my decisions and even from afar were always encouraging me and cheering me on.

To all my friends in Brazil, for giving me support even from so far away.

And finally, I thank my best friends in France, in particular: Giovana Pedroso, Arthur Finardi and Maria Eduarda Mariani, who I had the pleasure of meeting on this academic journey and who made it extraordinary.

Résumé

Aperam group

Aperam est une société sidérurgique luxembourgeoise, ancienne filiale d'ArcelorMittal, qui a été fondée en 2011. Est reconnue à l'échelle mondiale pour sa fabrication d'aciers inoxydables, électriques et spéciaux, et propose des services à plus de 40 pays. Ses activités se concentrent sur quatre domaines: Inoxydable & Acier Électrique, Services & Solutions, Alliages & Spécialités, et Recyclage & Renouvelables. Le groupe compte près de 11 000 collaborateurs répartis sur six sites de production au Brésil (Timóteo), en Belgique (Châtelet, Genk) et en France (Gueugnon, Imphy, Isbergues).

Sont des acteur majeur dans la collecte, le commerce, le traitement et le recyclage des déchets métallurgiques, avec une des empreintes carbone les plus faibles au monde, avec une production de 0,32 tonne de CO2 par tonne de brames

Le site d'Isbergues a été créé en 1881 par la Société des aciéries de France (fabricant de rails en acier). L'activité principale de ce site est la fabrication d'acier inoxydable, en particulier le laminage à froid, destiné aux secteurs industriel, automobile, pharmaceutique et chimique.

Le site couvre une superficie de 100 hectares et est composé de quatre sections : le centre de service et solution Aperam Stainless Service and Solution France, la ligne LC2I d'Aperam Stainless France, Recyco pour la collecte des déchets métallurgiques et le centre de recherche et d'innovation.

Au centre de recherche d'Isbergues environ 80 techniciens et ingénieurs travaillent, qui est organisé en quatre départements : Métallurgie et Soudage, Processus, Solution & Corrosion et Chimie. Les différents départements collaborent pour élaborer et créer de nouveaux produits métallurgiques, perfectionner les techniques de fabrication, proposer des solutions techniques et effectuer des analyses physico-chimiques.

Contexte général

Les aciers inoxydables sont composés d'une grande quantité de chrome (au moins 10,5 %) et de carbone (moins de 1,2 %). Ajouter dans la composition du nickel, du molybdène, du titane, du niobium, du manganèse et d'autres composants, permettra d'améliorer leur résistance à la corrosion et leurs caractéristiques mécaniques. Ils sont présents dans plusieurs domaines, comme les matériaux structuraux dans les bâtiments, les transports, l'industrie chimique et la vie quotidienne. Les quatre principales familles sont :

Ferritiques (α ou δ): grande résistance à l'oxydation à haute température et conductivité thermique élevée des ferriques. Utilisations : produits alimentaires, véhicules, infrastructures.

Austénitiques (γ): sont résistants à la corrosion, avec une grande ductilité, adhérence et forme, et possèdent de solides caractéristiques mécaniques. Applications dans la chimie, agroalimentaire, transport.

Martensitiques (α): résistance et dureté élevées, conductivité thermique élevée. Utilisée pour les outils de coupe, coutellerie, ressorts.

Duplex: combinaison de phases ferritiques et austénitiques, qui confère une grande résistance mécanique et à la corrosion. Applications : construction, le transport, l'équipement industriel, le traitement de l'eau et le secteur pétrolier et gazier. L' apparition des phases indésirables comme la phase sigma (σ) et les nitrures de chrome (Cr2N) dans le duplex peut avoir des conséquences sur leurs caractéristiques mécaniques et leur résistance à la corrosion. Est essentiel de surveiller attentivement leur traitement, notamment lors du soudage, afin d'éviter la formation de phases indésirables qui pourraient compromettre leurs performances.

Le soudage des aciers inoxydables duplex (DSS) nécessite une attention pour préserver les caractéristiques du matériau. Pendant l'opération de soudure, quatre zones sont identifiées : métal fondu (FZ), ligne de fusion, zone affectée par la chaleur ou HAZ et le métal de base. Les principaux défis sont d'équilibrer les phases austénitique et ferritique et d'éviter la précipitation des phases indésirables telles que les nitrures de chrome (Cr2N).

Un refroidissement trop lent ou rapide peut déséquilibrer la microstructure et ainsi affecter leur résistance mécanique ainsi que celle à la corrosion. Avant la soudure, la microstructure était plus fine avec environ 50% en volume de ferrite. Après soudure, il y a plus grosse microstructure dans les ZHA avec 70% maximum en volume de ferrite.

Pour minimiser ces risques, des simulations thermodynamiques on été fait à partir du logiciel Thermo-Calc pour optimiser la composition chimique des aciers inoxydables duplex et les essais thermomécaniques, avec la machine Gleeble 3800, on été fait pour optimiser la composition chimique ainsi que les cycles thermiques du soudage et pour garantir leurs propriétés après soudage.

Le principal objectif du projet consiste à réduire la teneur en ferrite dans les aciers duplex de 70%, conformément aux besoins des clients, afin d'éviter la formation de Cr2N, qui peut conduire à des problèmes de corrosion.

Il est possible de comparer les résultats de la simulation thermodynamique avec ceux obtenus par examen microscopique grâce à une analyse microstructurale permettant d'évaluer le passage d'une structure granulaire à une structure fine dans la zone affectée thermiquement (ZAT) après le soudage.

Metodologie

L'objectif du projet était de représenter et de surveiller la quantité de ferrite présente dans la zone HAZ des aciers inoxydables duplex après le soudage. Il a été possible de réaliser cette modélisation en combinant des simulations thermodynamiques avec le logiciel Thermo-Calc et des essais thermomécaniques avec la machine Gleeble 3800.

Les simulations en équilibre ont été effectuées à l'aide du logiciel Thermo-Calc, qui utilise la base de données TCFE9 Steels/Fe-Alloys 9.3, pour prédire la composition et le comportement des différentes phases dans les aciers inoxydables duplex. Les simulations se sont concentrées sur l'étude de l'influence des composés chimiques tels que le C, N, Si, V, Cr, Mn, Ni, Cu et Mo sur des paramètres essentiels : la température de début d'apparition de l'austénite (température A5), la température d'apparition des précipités de Cr2N (solvus Cr2N) et le pourcentage de ferrite à 1200°C. Il est crucial de respecter ces paramètres afin de prédire la microstructure après le soudage.

Une méthode a été mise au point afin de déterminer une formule de base pour diverses nuances de duplex, afin de simuler le comportement des composés chimiques. Deux techniques ont été employées : la première de vérification du comportement linéaire et la seconde d'extension de la gamme des compositions étudiées. Grâce à ces techniques, il a été possible de calculer des coefficients pour chaque élément et de vérifier la formule en effectuant des simulations accrues.

Les cycles thermiques de soudage ont été simulés à l'aide de la machine Gleeble 3800 sur des échantillons d'aciers inoxydables duplex. Des échantillons de différents niveaux ont été utilisés pour les essais, avec des dimensions précises (120-130 mm x 30 mm x 1,5-2,0 mm). Les essais ont été effectués à l'aide du modèle Rykalin 3D, qui simule les conditions thermiques tridimensionnelles présentes lors du soudage de plaques épaisses.

Les essais ont été réalisés avec des temps de refroidissement tr8-5 (refroidissement de 800°C à 500°C) de 10 et 20 secondes, en utilisant l'hélium pour un refroidissement rapide et l'air comprimé pour un refroidissement plus lent. Le température maximum a été de 1350°C afin d'éviter la fusion, et la vitesse de chauffage a été établie à 300°C/s afin de reproduire des conditions de soudage réelles. Pour évaluer les changements microstructuraux, des mesures de la vitesse de refroidissement autour de 1300°C et des analyses de courbes thermiques ont été réalisées avec l'aide d'une programme Python.

Après les essais Gleeble les échantillons ont été préparés pour une analyse microstructurale. Il était nécessaire de découper les échantillons de manière précise, de les polir afin d'obtenir une surface miroir, et de les attaquer chimiquement en utilisant le BERAHA pour colorer sélectivement les phases (ferrite rouge-marron et austénite blanche).

Les échantillons ont été examinés à l'aide d'un microscope optique afin de mesurer la quantité de ferrite présente dans la microstructure. Chaque échantillon a reçu trente photos à

partir de différents champs, et une analyse par seuillage manuel a été réalisée afin de mesurer la quantité de ferrite. Par la suite, les résultats obtenus ont été comparés aux prévisions effectuées par Thermo-Calc.

Résultats

Les simulations ont été très utiles pour prédire le comportement des aciers duplex lors du soudage, notamment pour la température de début d'apparition de l'austénite (point A5) et la température d'apparition des précipitations de Cr2N. Toutefois, on a constaté certaines incohérences, en particulier pour le grade DX2507 où la simulation ont la présence d'austénite dans le liquide, ce qui n'est pas conforme aux résultats expérimentaux. Cependant, ces résultats nous permettent de fixer une température maximale de 1350°C de test Gleeble.

Les résultats des essais Gleeble ont démontré une bonne stabilité, avec des fluctuations minimes dans les délais de refroidissement et les vitesses de refroidissement pour différents niveaux. Il a été confirmé par les résultats expérimentaux que les taux de ferrite après soudage étaient habituellement inférieurs à 70%, ce qui est nécessaire pour prévenir la formation de Cr2N. Cependant, on a constaté des fluctuations de température à environ 1300°C, ce qui a entraîné des modifications dans le système de refroidissement afin d'améliorer la précision des résultats.

L'analyse microstructurale a mis en évidence que les échantillons testés présentaient habituellement une microstructure essentiellement composée de ferrite après soudage, ce qui correspond aux prévisions de Thermo-Calc. Toutefois, des difficultés ont été observées avec le grade DX2507, où certaines zones n'ont pas présenté la microstructure grossière prévue après le traitement thermique. Des interrogations ont été posées quant à l'exactitude des conditions de test et à la pertinence des prédictions thermodynamiques pour ce grade particulier.

On a comparé les pourcentages de ferrite mesurés aux prévisions de Thermo-Calc, et même si les valeurs sont similaires, on a remarqué des différences, notamment pour le grade DX2507. Cela indique que, malgré sa puissance en tant qu'outil de modélisation, Thermo-Calc pourrait être sujet à des ajustements ou des calibrations supplémentaires pour certains types d'acier inoxydable duplex.

Conclusion

Au cours de ce stage, des progrès significatifs ont été réalisés dans la compréhension et l'optimisation de la teneur en ferrite dans les aciers inoxydables duplex, en particulier dans la zone affectée par la chaleur (ZAC) lors du soudage. Le thermo-Calc s'est révélé être un outil efficace et important pour les simulations thermodynamiques, permettant de prédire le comportement des aciers inoxydables duplex pendant le processus de soudage.

Bien que les simulations fournissent une approximation proche des paramètres importants, il est connu que les résultats de Thermo-Calc ne sont pas les mêmes que les valeurs mesurées, comme cela a été observé lors du projet avec l'analyse microstructurale. Cependant, après quelques tests, nous pouvons imaginer que peut-être les résultats de Thermo-Calc sont en réalité proches des valeurs réelles, en particulier avec le grade DX2507. Cela montre que certaines conditions doivent être modifiées afin d'atteindre une plus grande précision.

La machine Gleeble 3800 a été utilisée pour analyser et simuler les conditions de soudage ainsi que les effets des cycles thermiques sur la teneur en ferrite, de manière moins coûteuse et plus rapide. L'utilisation de cette machine permet d'optimiser la composition et les processus de soudage, ce qui a été validé par une forte corrélation observée dans la comparaison entre les résultats expérimentaux, l'analyse microstructurale et les données produites par Thermo-Calc. Cependant, certains problèmes, tels que le comportement inattendu du DX2507 et de légères variations dans les taux de refroidissement, indiquent que des ajustements supplémentaires sont nécessaires pour améliorer la précision et la fiabilité.

Enfin, après que les résultats ont été trouvés, certains points du projet doivent être améliorés. Par exemple : Pour la formule de base des différentes nuances de duplex, on peut conclure que certains éléments n'ont pas présenté un comportement linéaire dans la plage testée, il serait donc nécessaire de tester les termes quadratiques et les termes d'interaction. De plus, reconsidérer les conditions de travail avec le DX2507, peut-être en modifiant la température maximale du programme Gleeble, pourrait fournir des résultats plus précis.

Personnellement, travailler chez Aperam m'a apporté de nouvelles connaissances, notamment en métallurgie et plus précisément en acier inoxydable duplex. C'était ma première expérience dans ce domaine, et j'ai eu la chance de découvrir grâce à mon année chez Aperam, et cela m'a beaucoup plu. L'opportunité de travailler chez Aperam, en utilisant des outils de simulation avancés et des machines d'essai, a considérablement élargi mes compétences pratiques et ma compréhension dans ce domaine, offrant une solide base pour ma future carrière en ingénierie des matériaux.

Summary

Introduction

Duplex stainless steels (DSS) are recognized for their excellent mechanical properties and corrosion resistance, thanks to their fine balanced microstructure of ferrite and austenite of about 50% and thanks to their high chromium content greater than 20 %wt. Due to their relatively low nickel content, typically between 2 and 8 %wt, they also present a more stable price compared to austenitic stainless steels. However, the welding operation can alter these properties by changing the microstructure of the heat-affected zone (HAZ) and the chemical composition and microstructure of the molten zone (MZ).The welding parameters also play a significant role by changing the thermal cycle undergone by the various area of the weld. After welding, the microstructure becomes coarser and the ferrite rate can increase up to about 70-75% during arc welding operations and even reach 95% during laser welding, which can have a significant impact on the in-user properties of the steel.

In this context, it is critical to adhere to customer norms and specifications, including keeping ferrite content below 70%. This necessitates an accurate evaluation of the microstructure following welding, as well as modeling the ferrite content evolution based on chemical composition and welding conditions. The goal of this study is to assess and control these variables in order to ensure that welded Duplex stainless steels meet performance standards.

In this report, I will first present the company, with the entire group as well as some social and economic data. Then, to understand the subject of the internship, I will explain what stainless steel, duplex stainless steel, and finally, the duplex welding with the principle of heat-affected zone (HAZ). I will continue with the subject of the internship, the proposed missions and the presentation of the work carried out: thermodynamic simulations with Thermo-calc Software, Thermomechanical tests with Gleeble, Metallographic preparation and optical microscope analysis for ferrite rate determination and processing of Gleeble curves.

I. Company presentation [1]

A. Aperam group

Aperam is a Luxembourg-based steel company. Formerly a subsidiary of ArcelorMittal, Aperam was spun off in 2011 to become independent. Aperam is a world-renowned player in the production of stainless, electrical, and special steels, with customers in more than 40 countries. Since December 31, 2021, Aperam's activity is focused on four main sectors:

- Stainless & Electrical Steel;
- Services & Solutions;
- Alloys & Specialties;
- Recycling & Renewables.

Aperam is a leader in the production of high-value specialty products. The group's industrial network has nearly 11,000 people spread over 6 production sites:

Figure 1: Production sites of the Aperam Group

- Brazil (Timóteo);
- Belgium (Châtelet, Genk);
- France (Gueugnon, Imphy, Isbergue).

In 2022, Aperam exported 1.82 million tonnes of steel, enabling it to achieve a revenue of €5,102 million.

B. Aperam Isbergues

The Isbergues site was created in 1881 and developed by Société des Aciéries de France. Initially, this company specialized in the production of steel rails. Currently, the Aperam Isbergues site focuses mainly on stainless steel production. This site specializes in cold rolling and more generally in the production of products for the industrial, automotive, pharmaceutical and chemical industries.

The various certifications obtained by Aperam ensure the compliance of the various products (ISO 9001 and IATF 16949) but also the safety of personnel and the environment (ISO 14001, ISO 50001 and ISO 45001). The Isbergues site is classified as a high threshold SEVESO due to the storage of these different acids in large quantities.

The Aperam Isbergues industrial site employs around 400 people. Every day, the steel arrives at the site by train, but mainly by truck (about 1,000 tons per day). Then, generally, stainless steel is sold in coil form, as we can see in the image below:

Figure 2 : Photo of Aperam reels

Aperam Isbergues site extends over more than 100 hectares and consists of 4 branches:

- The Aperam Stainless Service and Solution France service center, which markets products in France;
- Aperam Stainless France with the LC2I line producing more than 280,000 tons of steel per year, also carries out treatments on stainless steel coils before their delivery;

- Recyco which is a unit for the recovery of waste and metallurgical by-products, using electric arc furnaces in order to reduce waste. It is also used to obtain new stainless steel raw materials to make new alloys;
- The research and innovation center studies steel compounds in order to improve the technology and quality of different steels, according to their fields.

C. Centre for Research and Innovation

The Isbergues research center has around 80 technicians and engineers. It is divided into 4 departments:

- Metallurgy and Welding: Ensures the design and development of new metallurgical products;
- Process: Development of new manufacturing methods and processes to improve production;
- Solution & Corrosion: In contact with the customer, offers different technical solutions for the design and forming of stainless steel, studies corrosion resistance and researches new solutions to develop new solutions surfaces by adding new properties;
- Chemistry: Carries out the various physico-chemical analyses, which allow the proper functioning of the studies carried out at the research center.

II. Prerequisites for understanding the internship

A. Stainless Steel [1, 2, 3]

Stainless steels are a group of iron-based high-alloy steels containing a minimum of 10.5% chromium, and less than 1.2% carbon. To improve its corrosion resistance and mechanical properties, nickel, molybdenum, titanium, niobium, manganese, and other components can be added to Stainless steel.

The term "stainless" comes from the fact that the presence of chromium will oxidize very quickly, forming a protective film, called a "passive layer" and constitutes a barrier against corrosion, whether localized or generalized.

The applications for stainless steel are numerous and varied. They are used as structural materials in buildings, transportation, the chemical industry (cooling systems, reactors, etc.), and everyday life (stoves, freezers, etc.).

The figure 3 is a Schaeffler diagram for stainless steel alloys, they are used to predict the microstructure of stainless steels based on their chemical composition, so to anticipate the phases that would exist depending on the alloy's composition. [3]

There are four main families of stainless steel: ferritics, austenitics, martensitics and duplex.

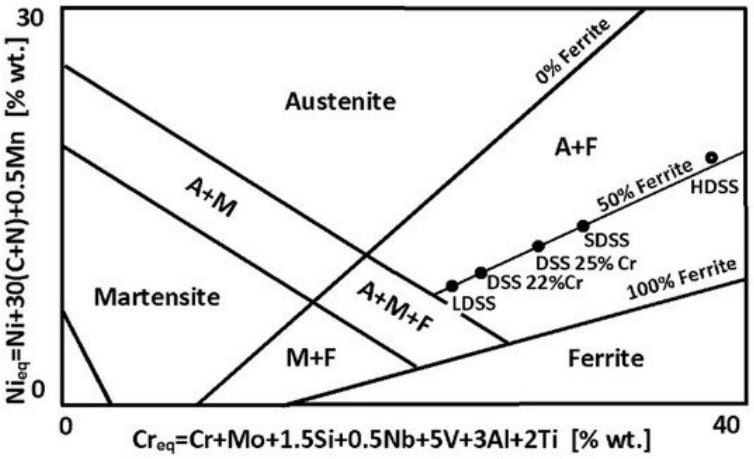

Figure 3 : Diagram for stainless steel alloys

I. Ferritics (α ou δ)

The composition of ferritic stainless steels is 10.5 - 30% chromium, 0.01 - 0.02% carbon and 0 - 4% molybdenum. Ferritics grades have an excellent high-temperature oxidation resistance and high thermal conductivity, ferritics expand less than austenitics when heated so they have lower thermal expansion, magnetic, good resistance to stress corrosion cracking, pitting corrosion and crevice corrosion.

Applications for ferritic stainless steel include commercial food equipment, automobiles, lifts, and building and construction.

II. Austenitics (γ)

Depending on the grade, its composition is 16-21% chromium, 6-26% nickel, low carbon (<0.1%) and can also contain molybdenum. Corrosion resistant in most environments; great ductility, weldability and formability; and strong mechanical qualities (low yield stress, relatively high tensile strength) are some of the benefits of these steels. They are also non-magnetizable and can be used in both hot and low temperatures thanks to this structure.

They are used in areas like chemical industry, food processing (milk cooler), tankers (shell and tank bottom), container shells, rail transport and for some industrial applications.

III. Martensitics

Martensitic stainless steels have 10.5-17% chromium and 0.2-0.5% carbon. These grades reach high resistance levels when hardened and tempered; at room temperature, martensitic stainless steel has excellent mechanical qualities that are on par with engineering steels and superior to those of duplex, ferritic, and austenitic stainless steels; has a thermal conductivity up to twice that of austenitic stainless steels and a thermal expansion coefficient roughly two-thirds that of austenitic grades, making it suitable for applications requiring dimensional stability under temperature changes even though it offers moderate to good corrosion resistance.

These properties make them suitable for a variety of applications, including cutlery, cutting tools, hand tools, and springs.

IV. Duplex

Duplex steel is a two-phase steel structure composed of ferrite and austenite that belongs to the austenitic-ferritic family. We are going to focus on duplex grades because this is the main focus of this work.

B. Duplex Stainless Steels [1, 2, 3, 4, 5, 6, 7, 8, 9]

Duplex stainless steels (austenitic-ferritic steels) contain both austenitic (γ) and ferritic (α) phases. They are formed from 21 - 26% chromium, 2 - 7% nickel, 0 - 4% molybdenum, 0.1 – 0.3% nitrogen and only 0.02% carbon. It is an appropriate balance between austenite-formers nickel & nitrogen and ferrite-formers chromium & molybdenum. The austenitic lattice facilitates toughness and ductility, whereas the ferritic phase offers strengthening.

Figure 4 : Duplex Stainless Steel before welding (metal base)

These steels have properties of both phases, such as good resistance to both stress corrosion cracking and intergranular corrosion, good mechanical strength, and a high yield strength coupled and maintains sufficient level of ductility (the ability to be stretched, extended, and lengthened without breaking), durability, formability, ease of use and low maintenance requirements.

Duplex stainless steel grades vary in corrosion performance based on alloy composition. There are several types of duplex:

- **Lean duplex:** without deliberate Mo addition, such as 2304 and 2202;
- **Standard duplex:** with around 22% Cr and 3% Mo, such as 2205 and 1803;
- **Super duplex:** with approximately 25% Cr and 3% Mo, such as 2507;
- **Hyper duplex:** with higher Cr and Mo contents than super duplex grades.

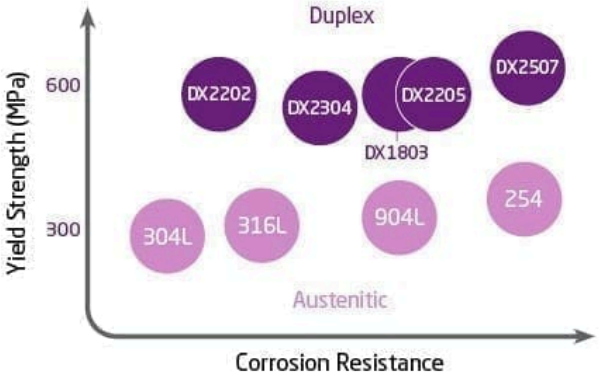

Figure 5 : Comparison of yield strength and corrosion resistance

Stainless steel's resistance to corrosion depends on its alloy content. So, the amount of alloy in stainless steel will determine its corrosion resistance. The main elements that affect pitting corrosion resistance are Cr, Mo, and N. The composition of stainless steel and its relative pitting resistance in solutions containing chlorides are related by an empirical connection known as the Pitting Resistance Equivalent Number (PREN). [6]

The PREN = Pitting Resistance Equivalent Number = %Cr + 3,3(%Mo + 0.5.%W) + 16.%N, where Cr, Mo, W, and N stand for the alloy's respective weight percentages of chromium, molybdenum, tungsten, and nitrogen. These elements significantly enhance the material's resistance to pitting corrosion. A higher PREN indicates better resistance to pitting, making these materials suitable for such applications.

- **Lean duplex:** PREN = 22-27, with a lower Ni content, are best for less severe environments;
- **Standard duplex:** PREN = 28–38, with 22%Cr and 3%Mo, it is mid-range in terms of corrosion resistance;
- **Super duplex:** PREN = 39–45, with25%Cr, 3.5% Mo and 0.22-0.3%N;
- **Hyper duplex:** PREN > 45 for severe environments.

Duplex stainless steels find use in the following industries: building and construction; transportation (cargo ships, tanker trucks, trains); equipment (tanks, pressure vessels, heat exchangers, tubes); desalination and water treatment (wastewater treatment, drinking water systems); and oil & gas (refinery, flexible, oil platform).

Figure 6 shows a Fe-Cr-Ni phase diagram for 70 weight percent Fe. The vertical dashed line in the phase diagram represents the composition of a potential DSS alloy. Ferrite and austenite precipitate in a fully-ferritic microstructure, causing the liquid to solidify. The ideal final microstructure for DSS is this ferritic-austenitic microstructure, achieving a phase balance close to a ratio of 50/50 [7].

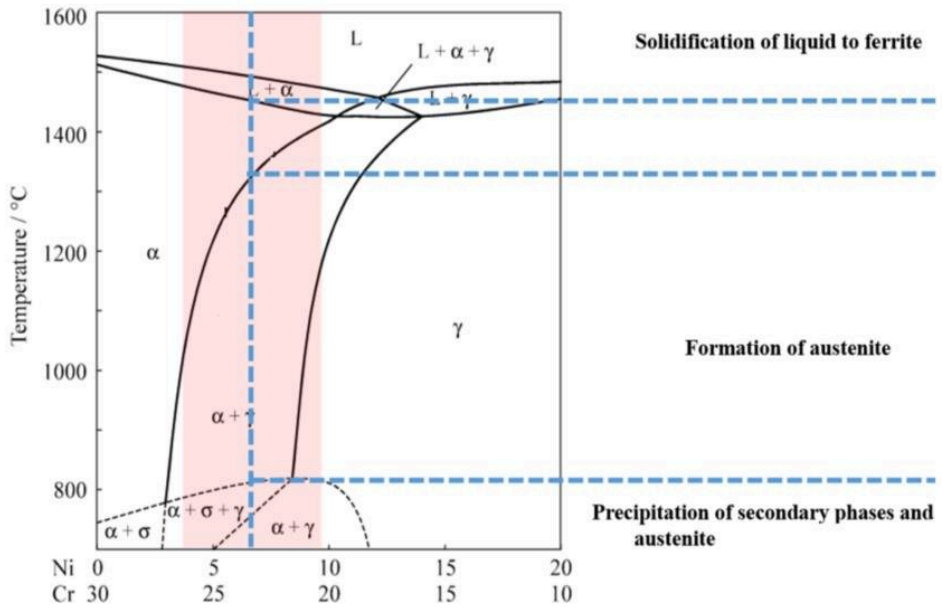

Figure 6 :Fe-Cr-Ni phase diagram for 70 wt.% Fe

DSS generally provides high resistance to both stress corrosion cracking and intergranular corrosion while keeping good mechanical properties. During cooling, around 1000°C to 550°C, precipitates of intermetallic phases are formed, as sigma phase and nitrate of chrome, as shown in figure 7 [8] which depends on the chemical composition, more alloy elements faster the precipitation.

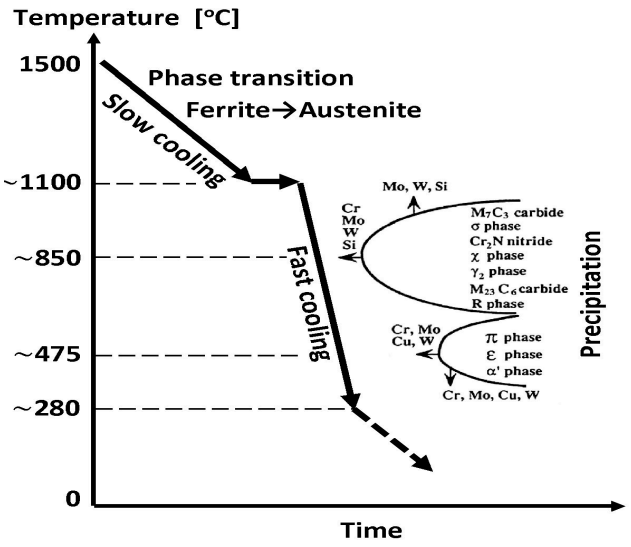

Figure 7 : TTT diagram (specified for the critical range only) typical for duplex steels. The arrows next to the symbols of the elements show the direction of the changes in the steel structure under the influence of that element.

DSSs are distinguished by two embrittling temperature ranges (C-shaped curves) where numerous secondary phases, carbides, and nitrides precipitate at varying holding durations. Figure 8 shows a representative TTT diagram for the grades 2304, 2205, and 2507. [9]

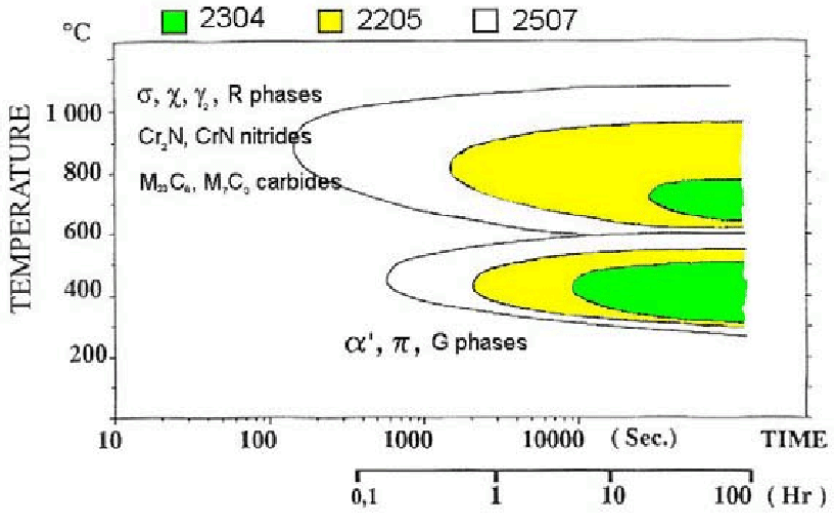

Figure 8 : TTT diagram showing the precipitation of different phases in for three different DSS

I. Sigma phase

The most significant intermetallic phase in stainless steel is the sigma phase (σ), which is chromium-rich. This phase depends on the thermal cycle and chemical composition. Because of its detrimental effects on the material's mechanical qualities and resistance to corrosion, this phase is undesirable.

The surrounding chromium metal becomes less resistant to pitting corrosion as a result of the production of these chromium-rich particles. In addition, these particles significantly reduce the impact toughness of the alloy at lower temperatures.

The sigma phase has a tetragonal unit cell (space group P42/mnm) containing 30 atoms. These atoms are located in five nonequivalent groups of inequivalent sites A, B, C, D, and E with the occupation numbers 2, 4, 8, 8, and 8,respectively. It is a structure that deforms a lot

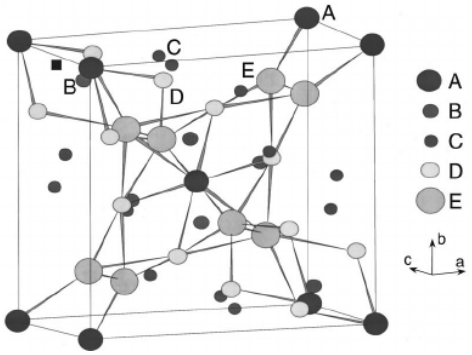

Figure 9 : Unit cell of the sigma phase

However, from the company's internal experience and after performing Gleeble tests with cooling times of 10 and 20 seconds, it can be concluded that there is no presence of sigma phase, as it's a fast cycle. Because of that, the chemical attack is used to identify the presence of ferrite, as there is no sigma phase.

II. Chromium nitrides

The Cr2N (Chromium nitrides), figure 10, is another phase that can form in duplex stainless steels and affect their mechanical and corrosion properties, which precipitate between 600°C and 1050°C.

This precipitation occurs because the ferrite becomes nitrogen-supersaturated due to a low solubility of nitrogen in the ferrite phase, resulting in austenite precipitation that transforms to Cr2N

and austenite deficient in chromium. It loses ductility, hardness, and corrosion resistance the more Cr2N there is in the material, making dissociation more difficult.

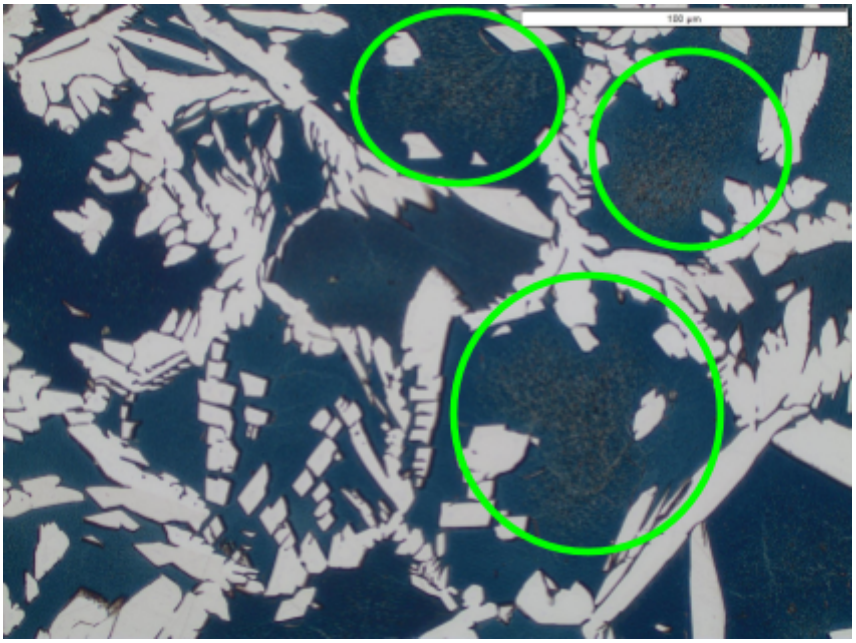

Figure 10 : Presence of Cr2N in the microstructure in the HAZ

As we can see in figure 11, which is a thermodynamic simulation made from the thermo-calc program, when Cr2N appears there is a change in the curve, so without Cr2N the austenite curve would increase. This precipitation in DSS is very important during the welding process.

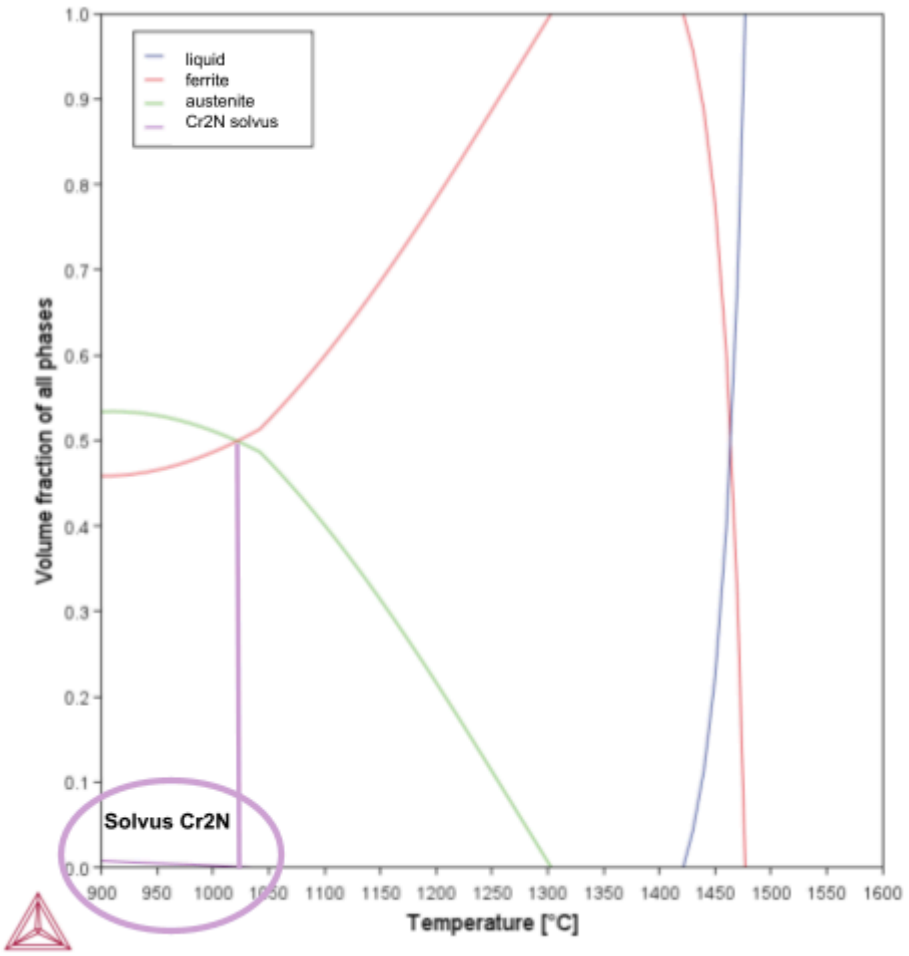

Figure 11 : Example of thermodynamic simulation showing the Cr2N precipitation

C. Welding Duplex Stainless Steels [4, 10, 11, 12]

The process of welding involves forging, heating the interfaces until the materials fuse together, or doing both at once to create a metal continuity between two sections. When a welded seam is seen in a situation where materials have fused together, four zones can be distinguished, as we can see in the figure 12:

1) The weld metal or fusion zone (FZ), is the part which melts during the welding process;

2) Melting line, which shares the melted and unmelted portions of the material;

3) Heat Affected Zone, or HAZ, where the temperature has caused metallurgical changes leading to different physical properties of the base material;

4) Base metal.

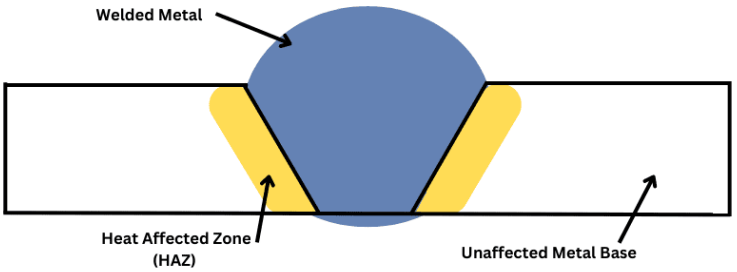

Figure 12 : Welding zones

Welding duplex stainless steels requires attention to several critical factors to avoid compromising the material's properties. There are two main problems that may arise during the welding, because of the change of the microstructure during the cooling: not having a well-balanced austenitic-ferritic ratio and the precipitation in the fusion zone and heat-affected zone (HAZ), and the toughness of the alloy.

To avoid difficulties in the HAZ, the welding process should include well-balanced cooling, neither too little nor too fast of this region following welding. Because too little heat input might result in extra ferrite in the melt zone or HAZ, so results in a loss of toughness and corrosion resistance, but an excessive heat input raises the possibility of intermetallic phase development.

Because of its fine microstructure and ferrite rate of around 50%, the unaffected base metal of Duplex Stainless Steel before welding offers superior mechanical and corrosion properties. However, due to welding operation (rapid heating and cooling to high temperature), the HAZ of DSS after welding will have a coarse microstructure and a ±70% ferrite rate, illustrated in figure 13.

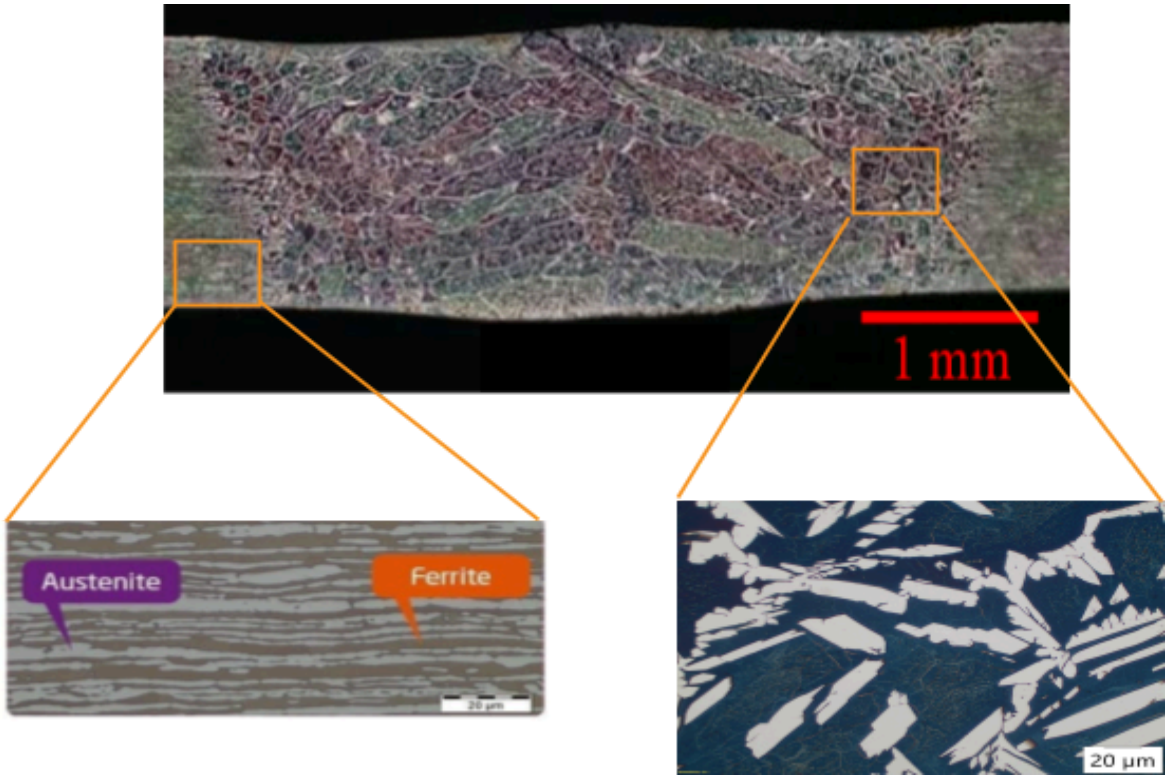

Figure 13 : Microstructure before (Fine microstructure) and after (Coarse microstructure) a welding process

Welding duplex stainless steels involves specific thermal cycles that directly influence the microstructures in the Heat Affected Zone (HAZ) of DSS and the mechanical and corrosion properties of the welded joints.

The figure 14 shows several distinct zones form due to the thermal cycle, such as [11]:

- Fusion Zone: A completely molten region where the substance forms into a ferrite and austenite mixture.
- Partially Melted Zone: Partially melting and solidification occur when the temperature approaches the melting point.
- Ferritic Grain Growth Zone: The high temperatures in the ferritic phase lead to significant grain growth. Reduced mechanical characteristics can result from grain development brought on by the high temperatures, particularly in the ferrite phase.
- Partial Transformation Zone: Rapid diffusion is made possible by high temperatures, which promotes the development of austenite grains. Large ferrite grains may generate side plates at grain boundaries upon rapid cooling.

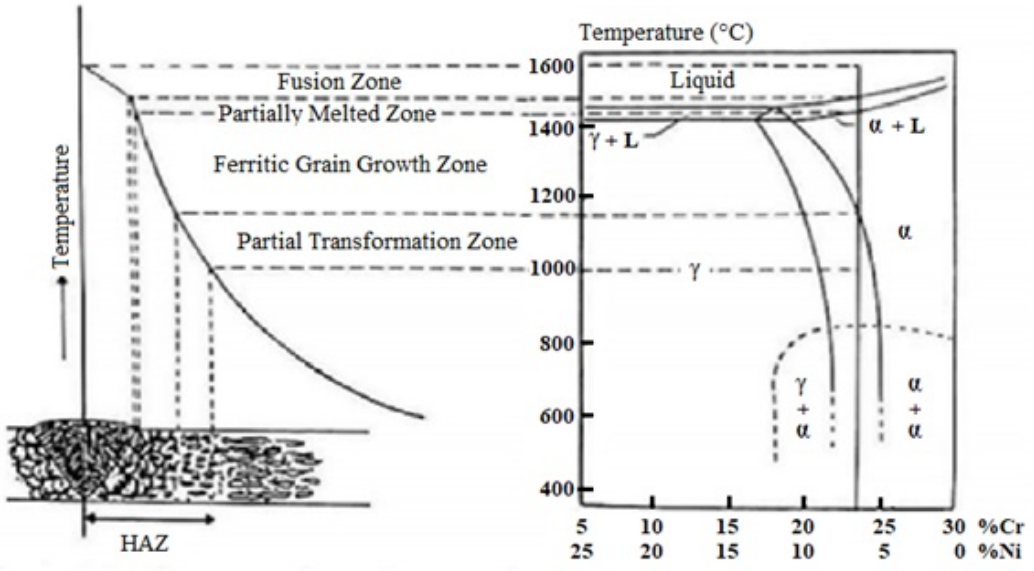

Figure 14 : Thermal Welding Cycle with Microstructures of HAZ for DSS

The thermal cycle can also be used to control the amount of austenite and nitride precipitation in the weld metal, which results in a greater amount of intergranular austenite because of the increased number of inclusions in the molten zone that promote the nucleation of this austenite [12].

D. Objectives

In order to continue projects previously started at Aperam, the goal of this study is to make sure that the ferrite content is below 70%, in compliance with customer standards and specifications. It is very important to have a ferrite percentage lower than 70% because if the rate exceeds this value there is a risk of forming Cr2N, as seen above, and then resulting in corrosion problems. For this, some programs and machines were used during the course of the project.

Thermo-calc software is used to make thermodynamic simulations, helping to improve the chemical composition of the different grades. With this improvement in composition it is possible to improve the weldability of Aperam products, and to guarantee the properties of those products. That is why a part of this project was looking for a basic formula for several nuances on the excel, to model an easier, cheaper and faster way to find the behavior of each element in the composition for the new DSS.

After that, thermomechanical simulations with the Gleeble 3800 machine is used to make the link between thermal parameters and microstructures, so the Gleeble are welding simulations, for the possibility of studying different thermal welding cycles with differents cooling time (10 and 20s). Some parameters are important to set in the program to have a result as close as possible to a real welding, such as heating speed and maximum temperature.

An important part of performing Gleeble tests is the analysis of the curves, seeing if they follow what the program has been told and to extract important information for the analysis, such as: Heating speed in °C/s between 200°C and 1200°C; Time in seconds between 800°C and 500°C (tr8-5), for the cooling time and speed in °C/s between 1275°C and 1325°C. To make it easier to find this data from the Gleeble results, a Python program was created.

Finally, a microstructural analysis with metallographic preparation and optical microscope analysis is done for the determination of the ferrite content. With that, compare the results obtained from the thermo-calc with the microscopic analysis. And also, to evaluate the change from a thin microstructure to a thick microstructure in the HAZ after welding.

III. Methodology

A. Thermo-calc [13]

I. Thermo-calc overview

Thermo-Calc is a comprehensive software tool that performs a variety of thermodynamic and property calculations which was developed by the Royal Institute of Technology of Stockholm (KTH). The software platform provides various built-in calculators that may be used to perform a variety of thermodynamic and property calculations, such as phase diagrams, property diagrams, Scheil solidification simulations, and more.

Thermo-Calc Software creates computational tools for predicting and understanding material properties, allowing you to generate computational materials data without expensive, time-consuming experiments or estimates based on restricted data.

In order to compare them with microstructural analyses and attempt to measure the impact of the elements on the phase fractions using a Ferrite rate modeling, and also to find a multilinear formula that fit Thermo-Calc, where in a first method is done in a smaller composition range but we have a rather linear comportament and after a second method that will increase this composition range and check if the formula works well, I used the thermodynamic simulation program Thermo-calc during my internship.

Those simulations are in equilibrium, so they use formulas to perform calculations. We know that in absolute values the results are not good, but the Thermo-calc results in relative values allow us to get closer in the real conditions, out of equilibrium.

II. Parameters and Results

The ThermoCalc 2024a with Database: TCFE9 Steels/ Fe-Alloys 9.3 was used to plot the equilibrium simulation graphs and to observe the effect of each element on the percentage of each phase. The elements chosen were: C, N, Si, V, Cr, Mn, Ni, Cu, Mo, illustrated at the appendix 2.

Initially, the equilibrium simulation graphs were plotted to assess the desired points, which are as follows: temperature A5, temperature of solvus Cr2N's initial appearance, and ferrite % at 1200°C; as we can see at figure 15.

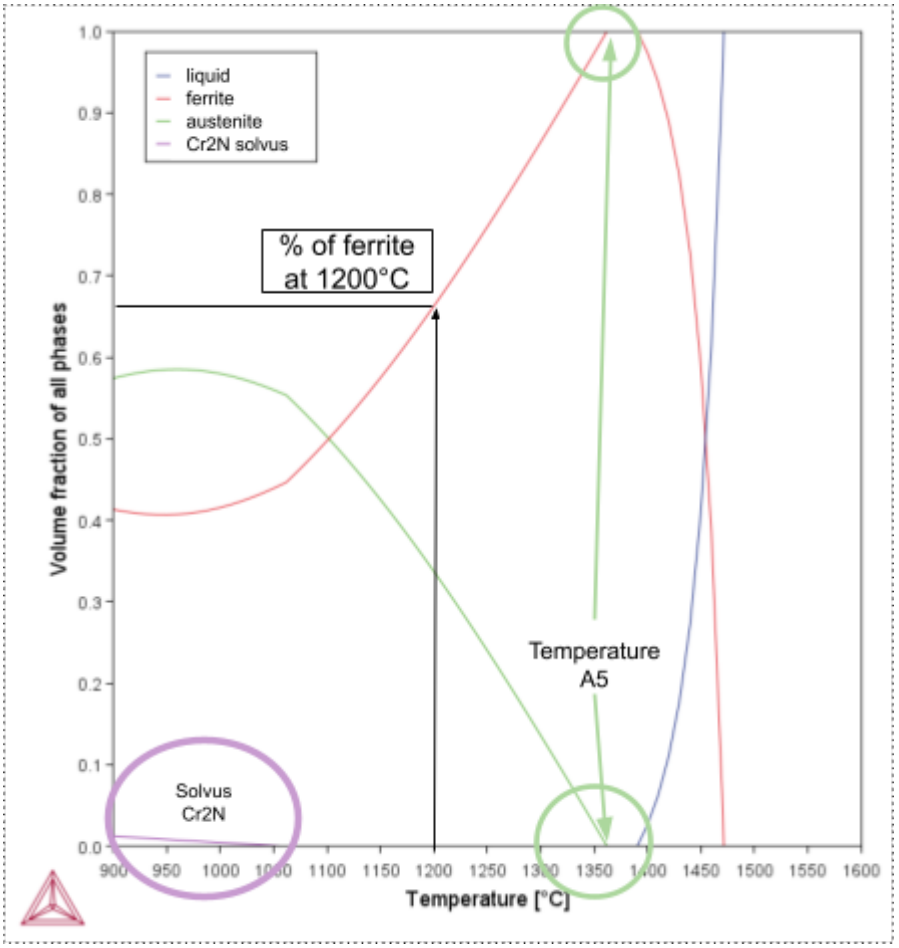

Figure 15 : Example of thermodynamic simulation showing the desired points

The ferrite rate is taken at 1200°C because it is close to the order of magnitude that is close to the real welding process, allowing us to see the evolution of the nuances.

The A5 temperature is when the first grains of austenite start to appear in the diagram. In figure 15 it can be seen that from this temperature the percentage of ferrite begins to decrease and that of austenite to increase. So when the cooling starts we will start to see austenite. We can also measure the temperature of A5 at the moment when the percentage of ferrite begins to decrease.

The initial temperature of the Cr2N solvus is the temperature of the first appearance of the precipitate in the microstructure, and is important to identify because it affects their mechanical and corrosion properties.

It is important to remember that these diagrams are not 100% faithful to what actually happens when heat treatment is performed, it is just an approximation. For example, in the diagram of a DX2507, figure 16, you can identify austenite in the liquid, but when the Gleeble tests are performed you can see that this does not happen because when we make the observations we have a coarse-grained zone, which is only possible to have it if we are 100% ferritic at a given time, which we cannot see in Figure 16 for example.

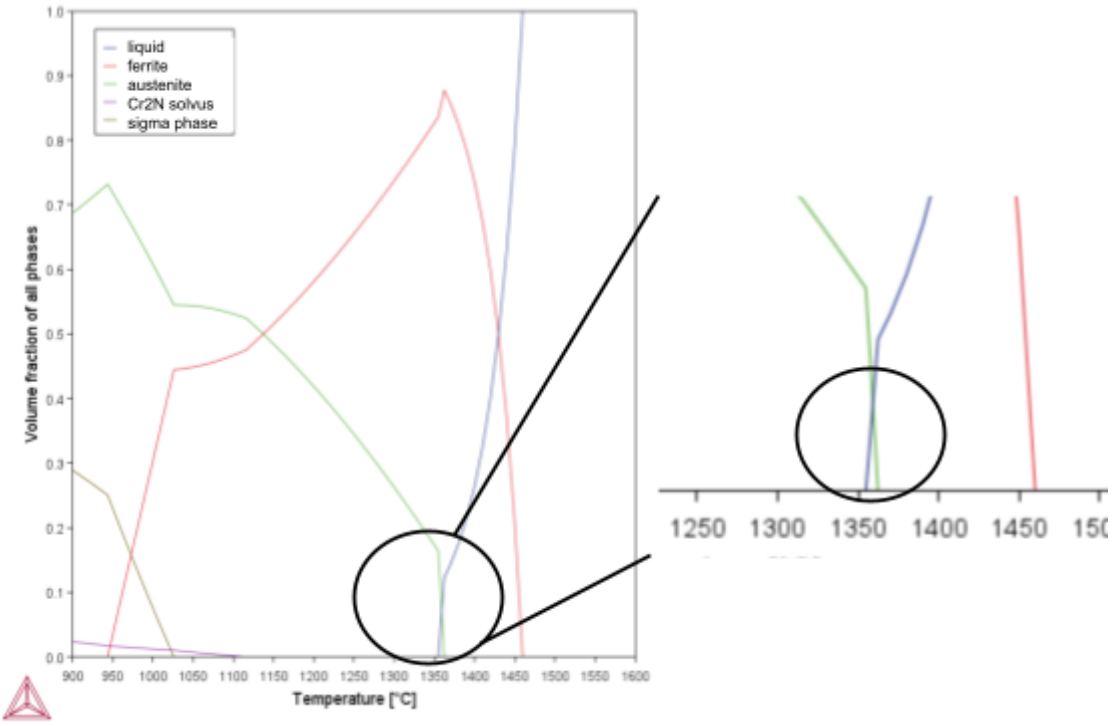

Figure 16 : Example of thermodynamic simulation of DX2507 showing the austenite (green) in the liquid (blue)

Another important step of the project was to find a base formula for different duplex classes to make it easier to identify the behavior of possible new compositions. Two methods were used to find this base formula. The first method allows us to check if we have a linear behavior and method 2 allows us to increase the range of worked compositions. Even if they are not very linear at the first method (appendix 3), the errors are quite small, so we can even consider them as a linear behavior.

The first method consists of finding a coefficient since one is looking for a lineaire formula, which makes a relationship between property and composition (formula 1). Each element varied at time with 3 points: average composition and +/- X% (between 5 and 20 depending on the elements).

After a Thermo-calc calculation, explained earlier, was launched to find the respectives temperature A5, temperature of solvus Cr2N's initial appearance, and ferrite % at 1200°C.

Formula 1: relationship between property and composition

$$property = constant + \sum . Ai . Ci$$

Where: Ai = Coefficient Ci = element

From this, the graphs temperature A5, temperature of solvus Cr2N's initial appearance, and ferrite % at 1200°C versus temperature were drawn to find the coefficient of each element for each of the desired points, as can be seen in figure 17. With this, it was possible to find a first formula, without the constant, with the coefficient (Ai) of the element (Ci).

With each first formula (without the constant) it's possible to find each constant for each formula, and then have a real formula. To find each constant, 1000 random compositions were made from excel with a percentage of variation for each element identified in table 1.

Table 1 - Percentage of variation in the composition of each element

delta compo (%)		10	10	10	20	5	10	5	20	20
Elements	Fe	C	N	Si	V	Cr	Mn	Ni	Cu	Mo

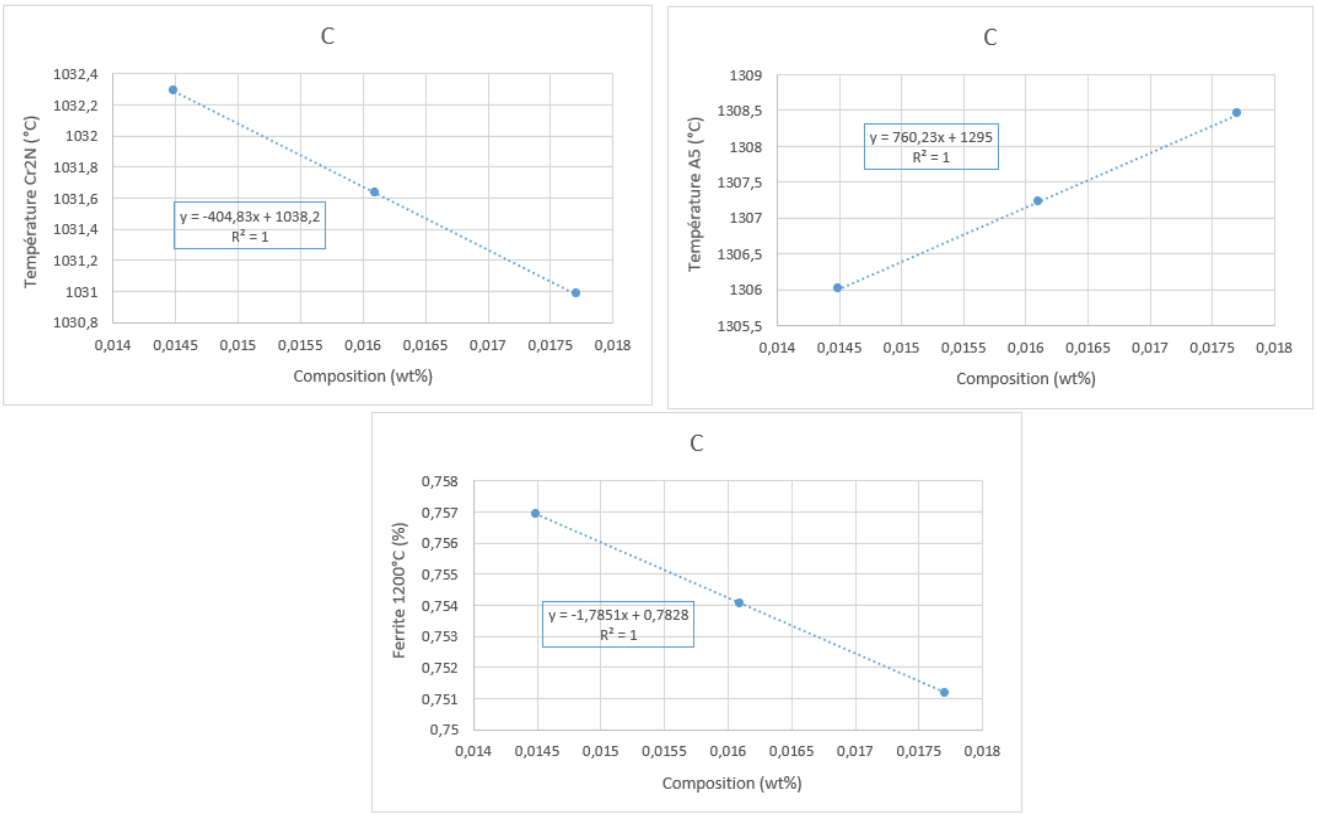

Figure 17 : Coefficient of C for the different desired points

Thermo-cal tests of these 1000 random compositions were performed to find the respective temperature A5, temperature of solvus Cr2N's initial appearance, and ferrite % at 1200°C of each of these 1000 compositions.

After that, the compositions were applied in this first formula (Ai*Ci) where each element was multiplied by its respective coefficient and then adding all these multiplications, which resulted in a value X. This value X will be subtracted from the found value of each temperature A5, temperature of solvus Cr2N's initial appearance, and ferrite % at 1200°C found in the thermo-calc. Finally, an average of these differences is made and this result is the constant of each formula.

In figure 18 we can identify the coefficients of each element, they are the result of Ai*Ci (multiplying each coefficient by its respective random composition). Delta corresponds to the difference between the temperature of Cr2N found by the thermo-calc and the formula Cr2N calculated in the next column and finally to the average of the delta column, resulting in the constant.

coeff formule T_CR2N								
a_CR2N_C	a_CR2N_N	a_CR2N_Si	a_CR2N_V	a_CR2N_Cr	a_CR2N_Mn	a_CR2N_Ni	a_CR2N_Cu	a_CR2N_Mo
-450,1285461	335,7311866	88,44812234	1112,070676	14,21359957	-7,16472595	-15,7651491	43,83068696	21,87108756
formula Cr2N	delta	average						
476,2035177	615,4478692	615,5756062						
449,9773329	616,509019							
445,4373854	615,6144664							
489,7904672	615,4120979							
481,3234142	615,6789338							
...	...							

Figure 18 : Example of method 1

As a second methode, the thermo-cal was used with the BATCH mode that performs the calculation of the solidus and liquidus temperature from random compositions generated by Excel with percentages of variations in chemical composition for each element, as can be identified in Table 1. This mode was used from 3000 random compositions.

For the batch mode to work the excel database provided must follow the format recommended by the help Thermocalc. At the appendix 4 we can see the table of each family, the % variation of each element, which follows the requested excel format.

From the results of the Batch mode, a synthesis of the data was performed (temperature A5, solvus temperature Cr2N and ferrite percentage at 1200°C) and, from a multilinear regression of excel it was possible to find an initial of a base formula for each result, and allows us to compare this formula generated by a linear regression of 3000 compositions with the formula obtained in method 1.This formula helps to model an easier, cheaper and faster way to find the behavior of each element in the composition for the new DSS with different compositions.

The nuances with the closest compositions and behaviors were grouped in the formula, which makes it possible to work on a wider range of possible new compositions. Are together: DX2304 + DX2202; DX2304 + DX2202 + DX2101; DX2205 + DX1803 (figure 19).

I tried to put the DX2507 in the graph below but it didn't work, it didn't turn linear. All the points come off the straight line, so we have a change in the slope. In addition, all points had a higher temperature of A5, with austenite present in the liquid, as shown at the thermo-calc diagrams.

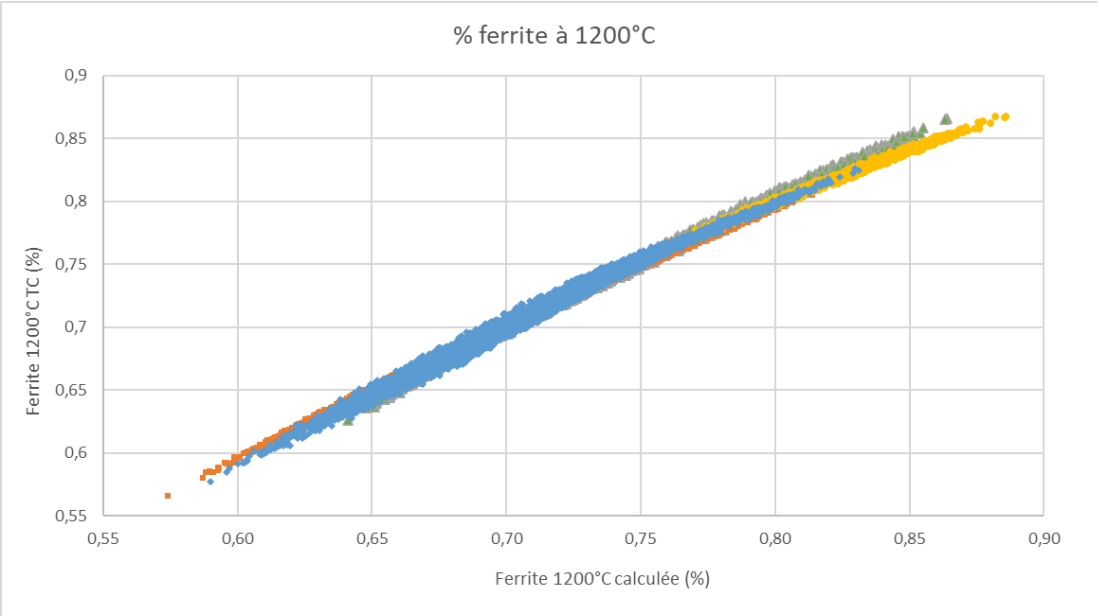

Figure 19 : Example of grouped compositions of DX2304 + DX2202 + DX2101

B. Gleeble [14, 15]

I. Gleeble Overview

Dynamic Systems Inc. (DSI) creates and produces machinery for process simulation and dynamic thermal-mechanical testing of materials. The Gleeble® System is the most well-known device made by DSI for physical simulation.

The machine is made up of different modules: an experiment module and a regulation module, associated with a computer with the software interface (Figure 20).

Typically, these machines are equipped with a computer control and data acquisition, system servo, hydraulic system, and high speed heating system, with a heating rate of 10,000ºC/s maximum. The heating of the sample is obtained by the Joule effect . With all those systems, it is possible to perform a wide variety of tests including HAZ simulation, such as the machine is capable of heat and cool quickly or slowly in accordance with regulation, maintain a temperature, and deform according to different modes.

To replicate the thermal cycling of a heat-affected zone is used a software called "QuicksimTM Software Heat Affected zone" that is offered by DSI. As the first step it is necessary to program a thermal cycle using several models and parameters with this software/interface.

Gleeble is used because you can change the parameters easily, performing several tests with different parameters quickly, so the possibility to make a large range of parameters. And also look at a single area in an easier way because it's bigger, unlike welding where we look at a large area, it is difficult to see a certain area, which is the case of HAZ.

Figure 20 : Overview of the Gleeble 3800

II. Parameters

The model used in these experiments is called RYKALIN 3D, and it was used because Aperam wants to develop thicker grades (between 10-12mm), for that we have to do bead on plate tests in the sheet, so we will vary the welding energy, remaining the same flow mode. The bead on plate is 3D on thick sheet metal, so the 3D is used at the Gleeble to compare bead on plate tests with comparable conditions

The three-dimensional thermal conduction equation, which explains how heat moves through a material, is the foundation of the Rykalin 3D model. By analyzing the temperature distribution brought on by a moving heat source over a workpiece, Rykaline's equation, which gives the relationship between temperature and time, accurately captures the speed of thermal

cycles measured in real-world situations. This equation is used to analyze the thermal effects in welding processes.

For the test, the samples used were measuring 120-130 mm in the rolling direction X 30 mm in the transverse direction X 1.5 - 2.0 mm thickness. They were cut from the guillotine shear and after they needed to be deburred.

The sample is positioned within copper jaws, which are situated within water-cooled jaws (Figure 21). The reason copper jaws are used is that they improve sample cooling, they are better thermal conductors and they are excellent electrical conductors, it allows you to reach the speed of rising in higher temperatures.

The quenching system is situated on either side of the sample, and they are composed of tubes with holes drilled through. Neither inerting nor vacuuming occurs.

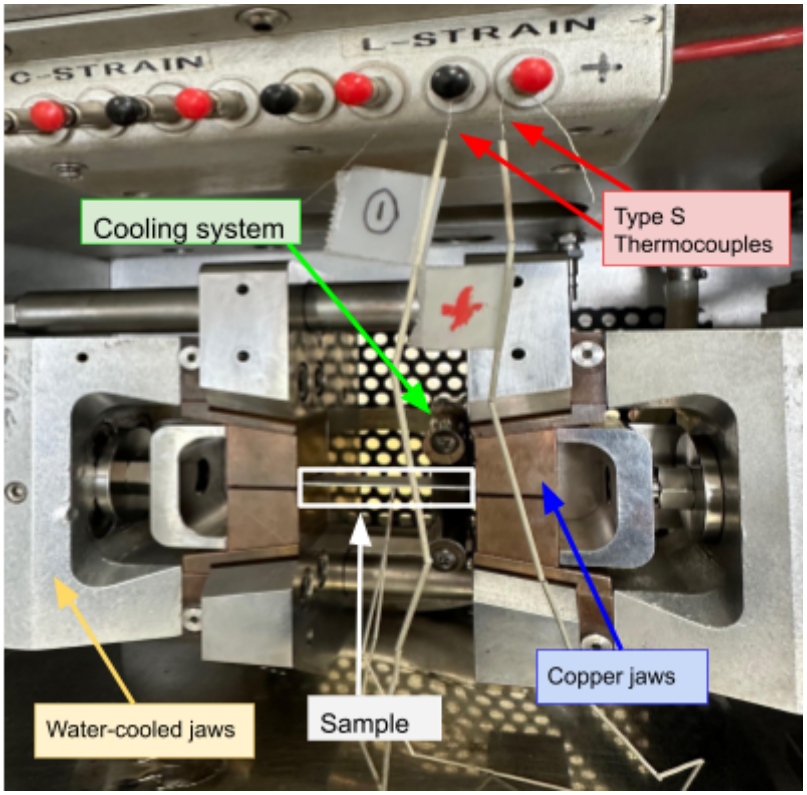

Figure 21 : Test chamber Gleeble 3800

Type S thermocouples are used because they withstand high temperatures (up to about 1600°C). They should be placed right in the center of the sample because the medium is the hottest zone of the sample, aligned and close together, as shown in figure 22.

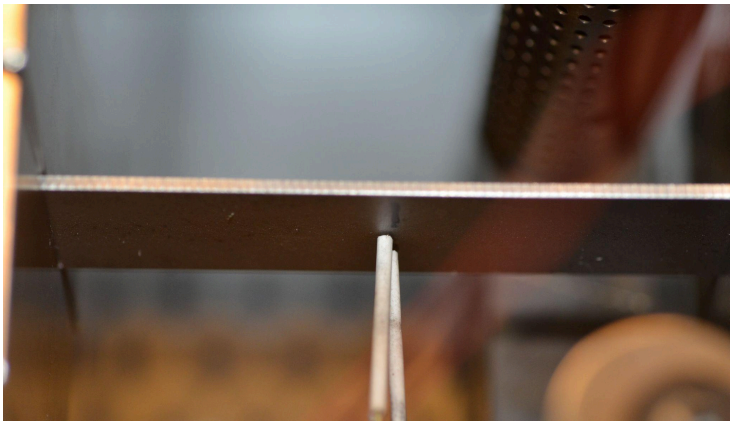

Figure 22 : Thermocouple well placed

The thermal cycle in Figure 23, there are two curves that can be identified: the blue one identifies as PTemp that corresponds to the program that was sent to the system, that is, what is expected as a result; while the orange curve is the result, which was carried out in the test.

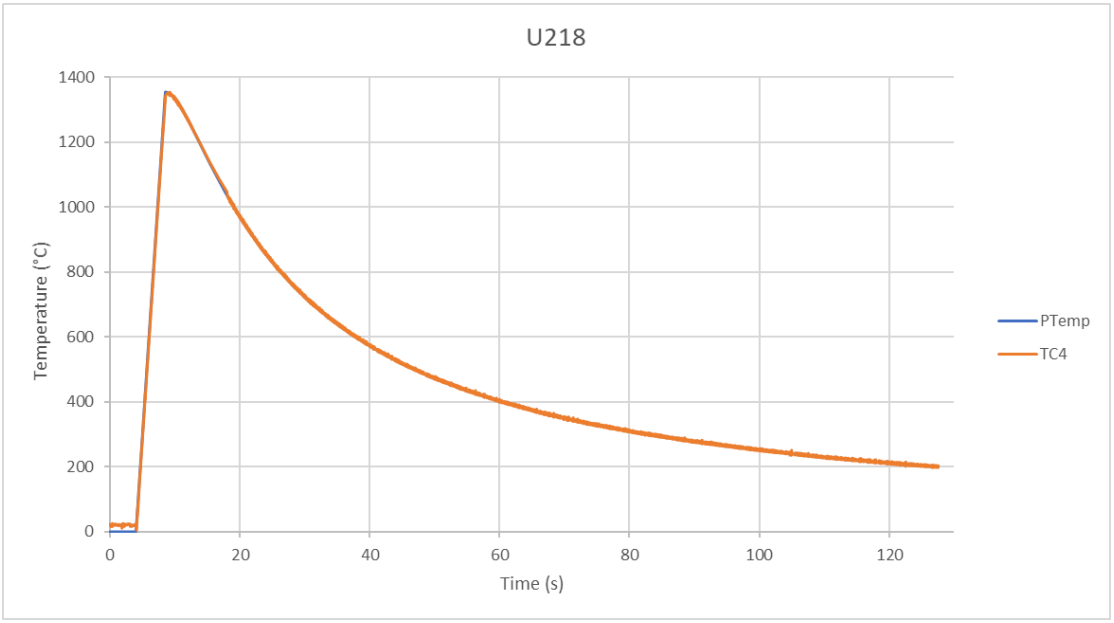

Figure 23 : Example of used thermal cycle (tr8-5= 20s)

The project involves using a Gleeble 3800 to simulate various welding temperature cycles, or variations in cooling times (tr8-5 = 10s and 20s) between 800°C and 500°C, using Helium and/or compressed air, and to determine the maximum temperature (Tm) so that a curve analysis can be performed (figure 23).

The tr8-5 is the cooling time of the curve. Its chosen tr8-5 = 10s and 20s because they approximate TIG and MAG welding, they are within the application range of arc welding. The tr8-5 is a conventional reference from carbon steels. In the duplex it is useless because the phase transformations are at high temperatures (between 1000-1300°C), that is why we look at the cooling rate at 1300°C.

For the cooling time of 10s is needed a rapid cooling, so the helium is used at first, because of his calorific value which is higher than compressed air, so it is more efficiently and, after 500°C, compressed air its used due to economic reasons and because from this temperature there is no more metallurgical transformation. However, for a cooling time of 20s, the compressed air can perform cooling because it is not necessary for it to be extremely fast.

The maximum temperature (Tm) chosen is 1350°C because it is a temperature higher than the expected temperature of A5 and lower than the temperature that will melt the sample. And it involves a heating speed of 300°C/s because this is the value that can be used for several thicknesses without having experimental problems.

III. Results

Tests were carried out with the nuances DX2101, DX2304 and DX2507, with the composition shown below in table 2.

Table 2 - Composition of different grades

grade	coil number	C (%)	N (%)	Si (%)	V (%)	Cr (%)	Mn (%)	Ni (%)	Cu (%)	Mo (%)
DX2101	30xxxxxx	0,0217	0,2202	0,77	0,073	21,72	5,36	1,66	0,23	0,39
DX2304+	02xxxxxx	0,0135	0,1594	0,44	0,11	23,65	1,55	4,48	0,38	0,61
DX2507	20xxxxxx	0,0095	0,2800	0,30	0,063	25,71	0,78	7,30	0,27	3,73
DX2507	94xxxxxx	0,0158	0,2657	0,39	0,091	25,71	0,82	6,66	0,32	3,73

Ten samples of each coil were tested, 5 samples with a cooling time of 10s and the other 5 in 20s. This was done to confirm the repetition of the values and thus predict a range of values that we can obtain from the results for each grade.

The Gleeble test results in a curve, as seen previously, that shows the thermal cycle performed. The figures 24 represent examples of Gleeble curves of 10s and 20s cooling time of samples that were analyzed.

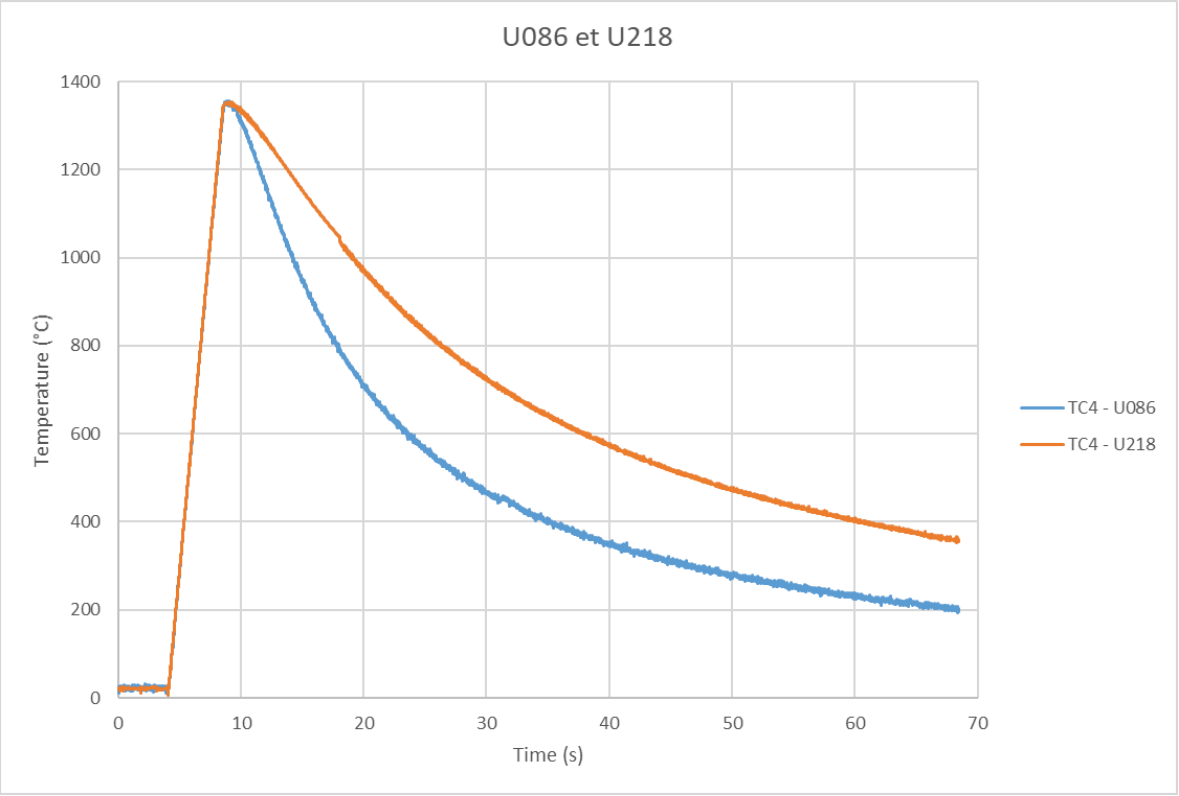

Figure 24: In bleu: Thermal cycle tr8-5= 10s sample U086

And in orange: thermal cycle tr8-5= 20s sample U218

From these curves, a range of values can be identified for the data to be analyzed. For example, the maximum temperature for a tr8-5 of 10s ranges between 1350-1363°C. While for tr8-5 of 20s it varies between 1350-1365°C.

We aimed for a tr8-5 equal to 10 or 20s and as a result we obtained the values shown in table 3. We can see with table 3 that the trials are well reproductive, and are similar.

Table 3- Tr8-50 results

grade	Tr8-5 = 10s (max and min)	Tr8-5 = 20s (max and min)
DX2101	Tr8-5 min = 10,12s Tr8-5 max = 10,6s	Tr8-5 min = 20,49s Tr8-5 max = 20,9s
DX2304+	Tr8-5 min = 10,18s Tr8-5 max = 10,52s	Tr8-5 min = 20,13s Tr8-5 max = 20,95s
DX2507. A	Tests not done	Tr8-5 min = 20,59s Tr8-5 max = 21,0s
DX2507. B	Tests not done	Tr8-5 min = 20,52s Tr8-5 max = 20,75s

In all tests conducted between DX2101, DX2304+, DX2507.A and DX2507.B the heating rate was always between 294-300°C/s.

Table 4 shows the cooling rate at 1300°C minimum and maximum, which is calculated between 1275 and 1325°C. It is calculated in this interval because around 1300°C is when the microstructure undergoes a change, there is a phase transformation. We can see that for tr8-5 = 10s the values are less homogeneous than for tr8-5 = 20s.

Table 4 - Difference between cooling rates at 1300°C

grade	Cooling rate between 1275°C and 1325°C Tr8-5 = 10s	Cooling rate between 1275°C and 1325°C Tr8-5 = 20s
DX2101	Cooling rate min = 29,67°C/s Cooling rate max = 59,14°C/s	Cooling rate min = 20,59°C/s Cooling rate max = 30,29°C/s
DX2304+	Cooling rate min = 36,20°C/s Cooling rate max = 60,67°C/s	Cooling rate min = 33,18°C/s Cooling rate max = 35,79°C/s
DX2507. A	Tests not done	Cooling rate min = 28,55°C/s Cooling rate max = 32,57°C/s
DX2507. B	Tests not done	Cooling rate min = 32,34°C/s Cooling rate max = 32,51°C/s

It is notable at figure 23 that the curve is not completely smooth, but there is a variation. This variation is considered negligible since it is about 5°C in an extremely fast time interval.

The figure 25 shows in a more enlarged way two points to be analyzed, in image (a) it is possible to identify the maximum temperature reached during the test and in (b) it is possible to find the tr8-5 result of the test.

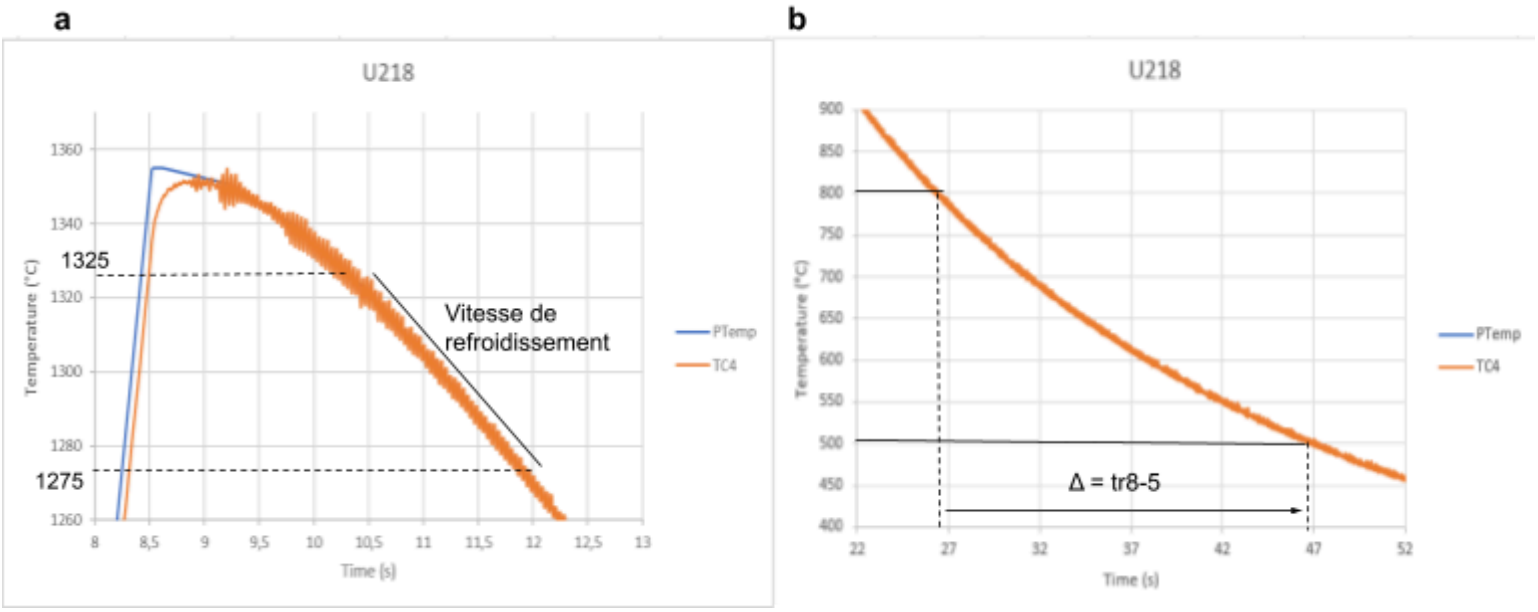

Figure 25 : Thermal cycle tr8-5= 20s sample U218. (a) maximum temperature; (b) Tr8-5

After performing Gleeble tests it is necessary to analyze the curves, seeing if they follow what the program has been told and to extract important information for the analysis. For that a Python program (appendix 5).

The Python program takes the Gleeble results, it smooths the curve, to reduces the irregularities/variation of the Gleeble curves, and then answer the following points: Heating speed in °C/s between 200°C and 1200°C; Time in seconds between 800°C and 500°C (tr8-5), for the cooling time and speed in °C/s between 1275°C and 1325°C, as seen at figure 26. These points are important for us to be able to compare them with real welds, to identify phase transformation, and for the development of new compositions.

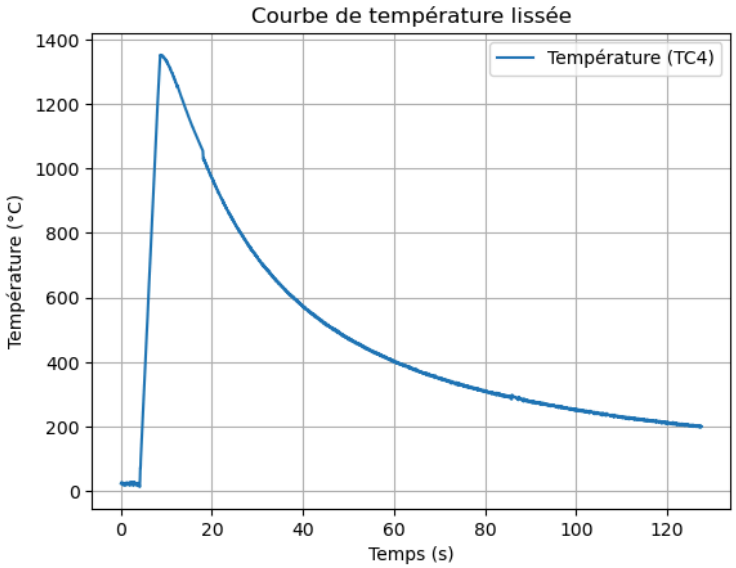


```
Température maximale (TC4) : 1352.5103000000001 °C
Vitesse de chauffage en °C/s entre 200°C et 1200°C (valeurs avant d'atteindre la température maximale) : 298.5079610778443 °C/s
Temps en secondes entre les températures les plus proches de 800°C et 500°C après avoir atteint la température maximale: 20.54
s
Vitesse en °C/s entre 1275°C et 1325°C (après avoir atteint la température maximale) : 31.01126250000008 °C/s
Temps total pendant lequel la température est supérieure à 1000°C: 11.66 secondes
Temps total pendant lequel la température est supérieure à 1100°C: 8.89 secondes
Temps total pendant lequel la température est supérieure à 1200°C: 5.76 secondes
Temps total où la température reste au maximum (PTemp): 0.03999999999999915 secondes
```

Figure 26 : Python program results

C. Microstructural analysis

After performing the Gleeble tests and checking the curves, the samples undergo a preparation so that they can be evaluated to determine the phase proportion of ferrite present. Abrasive cutting, polishing, chemical attack and observation under the microscope are part of the missions of my position and a clearance and training are required to be able to manipulate the tools mentioned above.

As a first step, the Gleeble samples are cut in Buehler Samplmet Cutter (appendix 6). For this project, the cuts are made by the area that has undergone thermal treatment with Gleeble, the darkest area of the sample, as we can see in sample A of figure 27.

After that, Secotom Precision Cutting Machine (appendix 7) is used from sample B in figure 27, because it cuts with a lot of precision. The cut needs to be closer to the thermocouples, which is the area of interest because it is HAZ, a zone where the temperature has been controlled by thermocouples, resulting in the sample C.

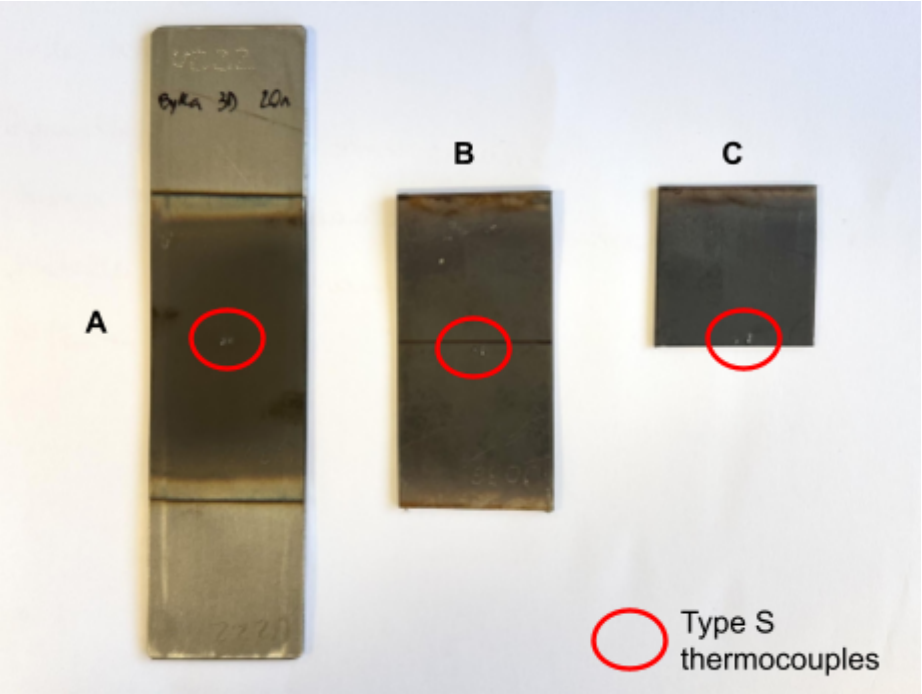

Figure 27 : Test tube after polishing and before attack

After the cutting steps mentioned above, sample C will undergo polishing on the Struers LaboForce-100 (appendix 8). A force is applied on the sample holder, the samples are polished with SiC paper, P80 to P1200, with the presence of water to prevent the sample from heating up, from grains ranging in size from larger to finer. Then with polishing cloth from 6 to 1µm, with a diamond paste and lubricant are used to avoid the heating up. The objective is a "shinier" surface, with a clean mirror without scratches to obtain a better result from the observations under the optical microscope.

In the last step before observations under the optical microscope, the samples are attacked chemically by being submerged in a BERAHA reagent solution. The components of the BERAHA attack are 0.28g of potassium metabisulphite ($K_2O_5S_2$), 19 mL of hydrochloric acid (HCl), and 100 mL of distilled water. This attack colors ferrite brown-blue and leaves austenite white, allowing for great contrast for the phase quantification, as we can see in figure 28.

Figure 28 : Observation under the microscope, ferrite brown-blue and leaves austenite white

Finally, if the attack was as expected, the observations are performed on the Olympus GX71 microscope. To determine the amount of ferrite present, 30 photos of different fields must be taken with an x500 magnification and, after that, the manual thresholding of those fields. The percentage of ferrite present in each photo will be calculated and after that the average of these 30 photos will be used. (Figure 29).

(a) (b)

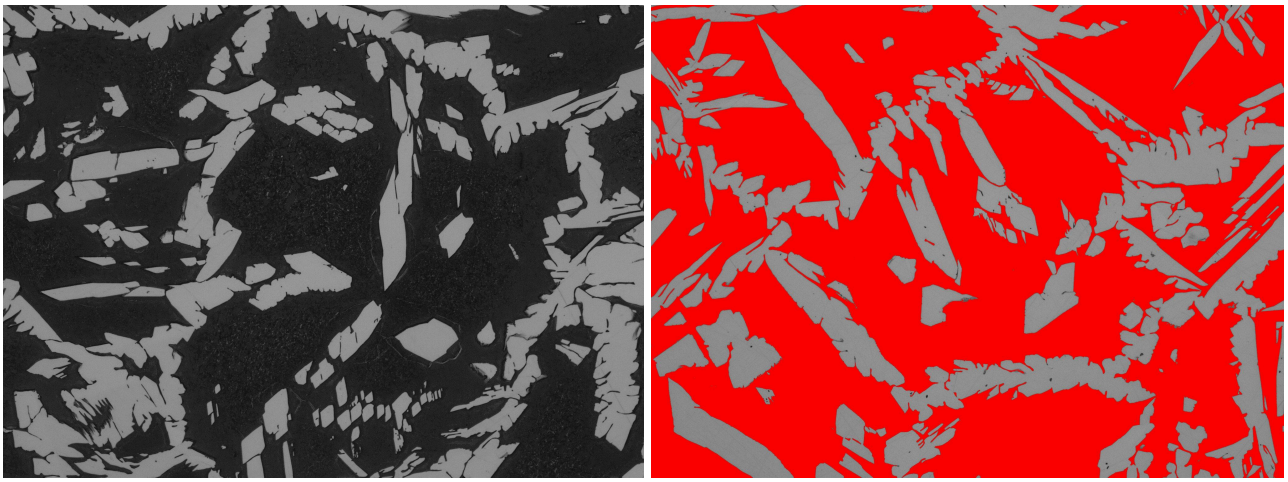

Figure 29: Observation under the microscope, (a) photo of the field to be analyzed; (b) photo of the thresholding of the field

IV. Results

In this part I will explain in more detail how to bring critical analysis in the data provided in the methodological part and, in addition, bring some problems faced during the project.

A. Gleeble + Microstructure results

From the Gleeble results, the analysis of the Gleeble curves and the microstructural analysis performed, it is possible to draw the graphs of ferrite percentage versus tr8-5.

In figure 30 there is a graph of ferrite percentage versus tr8-5 (10 and 20s) of a DX2304+. From this graph we can see that the range of the percentage of measured ferrite does not have a large dispersion, the results are close, and this happens for the other grades as well. Therefore, it can be said that the repeatability of the values is good, with a small difference between the values. In addition, we see that the experimental tr8-5 values, results of the analysis of the curves, also have repetition of values.

Those values come from the microstructural analysis that was performed on Gleeble samples. It is worth remembering that there is a difference in errors between each analysis.

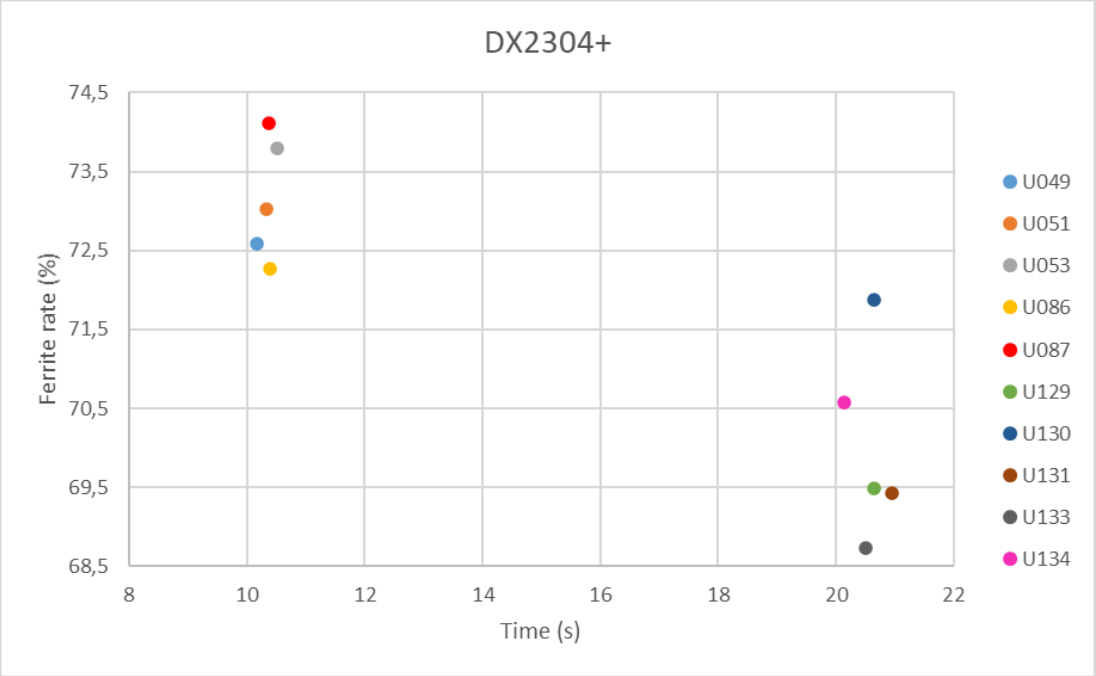

Figure 30: Graph of ferrite percentage versus tr8-5 (10 and 20s) of a DX2304+

After this, a second graph was drawn of the percentage of ferrite versus the cooling rate. We can see that for the samples that were tested with a tr8-5 = 10s (U049, U051, U053, U086, U087), that the cooling rate are not homogeneous, so the repeatability of this data is not so good.

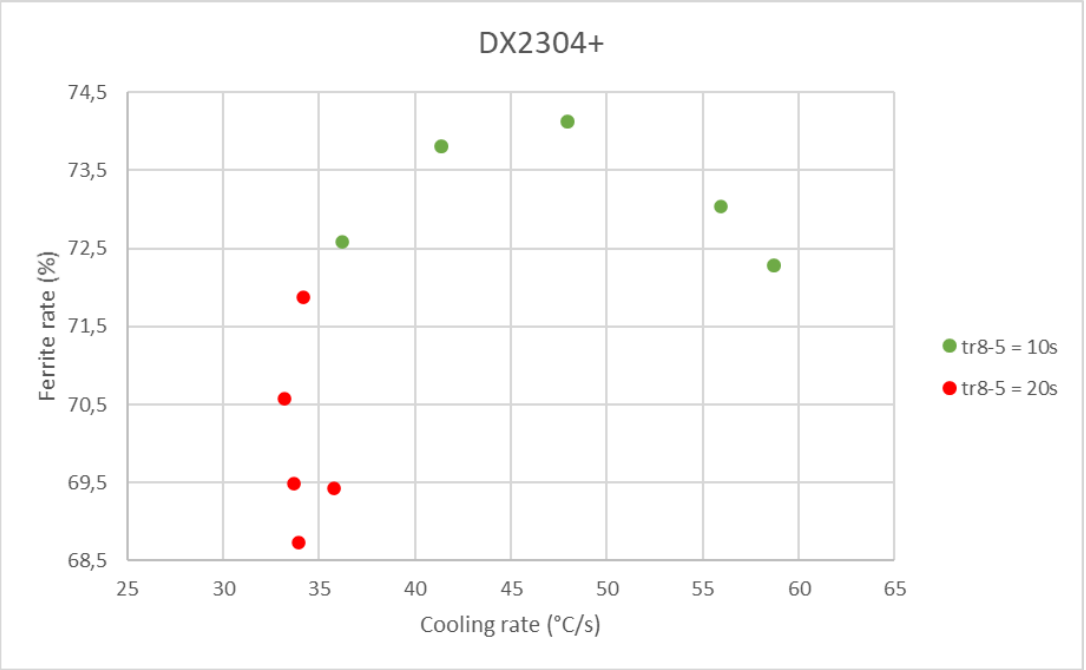

Figure 31: Graph of ferrite percentage cooling rate at 1300°C (°C/s) of a DX2304+

Whereas in figure 32, it is an average of the ferrite percentages per grade for tr8-5 of 10 and 20s. There are values that are missing from the graph, because as we will see in the next section, during the microstructural analysis of DX2507 problems were found, where we saw that the microstructure found during the analysis does not seem to have undergone heat treatments, the microstructure remained fine and still presents a banded microstructure.

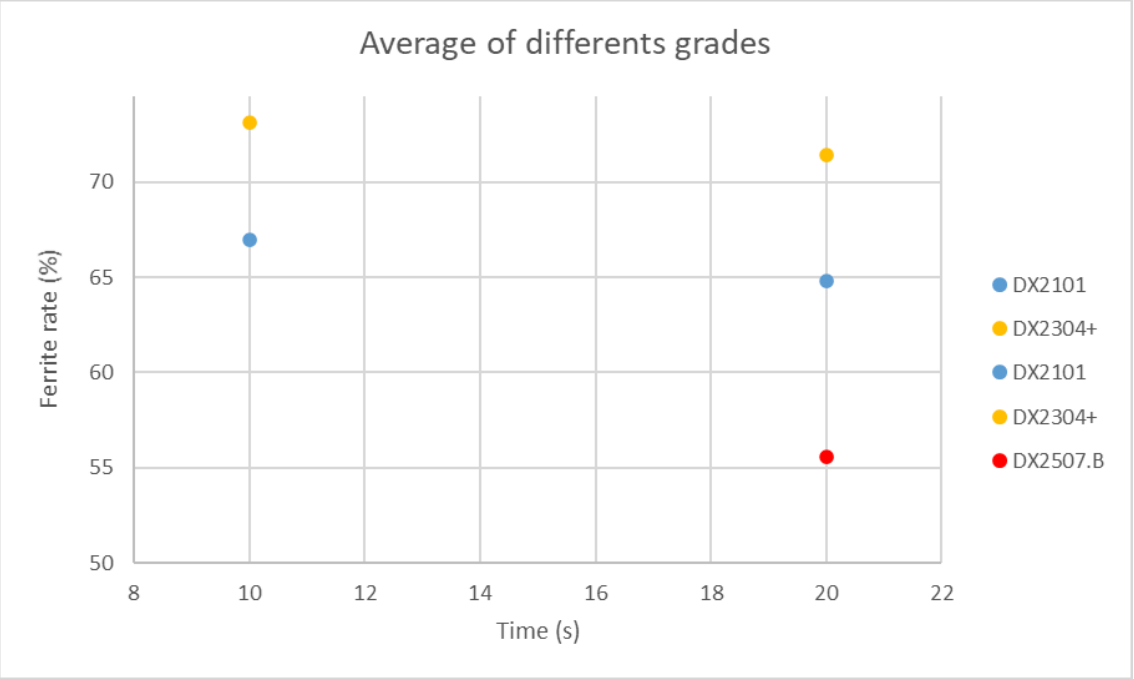

Figure 32: Graph of the average ferrite fraction versus tr8-5 (10 s and 20 s). Average of 5 samples except for DX2507.B 2 samples

After making the graph present in figure 32, it was possible to compare the results obtained experimentally with the percentage of ferrite provided by thermo-calc, and it can be concluded that there is a proximity between the values, and that the range of values is not so large, as we can see at table 6.

Table 6: Ferrite percentage difference between Thermo-Calc and the measured value

Grade	Thermo-calc	Measured (tr8-5 = 10s)	Measured (tr8-5 = 20s)
DX2101	72%	66%	65%
DX2304+	71%	73%	70%
DX2507.B	58%	test not done	56%

B. Experimental issue and discussion DX2507 results

The project began with the thermodynamic simulation program Thermo-calc. At first, it was possible to determine the values of the percentage of ferrite at 1200°C, the temperature of point A5 and the temperature of solvus Cr2N's initial appearance. The results of those points that are

represented in appendix 9, allow us to have an idea of the behavior of the composition of each type of duplex that we work with. These values also allowed us to determine a maximum reference temperature to put in the Gleeble test program, of 1350°C as mentioned before, which is a high temperature but before melting.

Even though it gives us a good prediction of DSS behavior, thermo-calc has some inconsistencies. One of them is the temperature value of point A5, the first appearance of the solvus Cr2N. Especially in the DX2507 grade, it is possible to identify the presence of austenite in the liquid, as previously illustrated in figure 16, which is known to be not consistent with the reality of the tests.

Although these DX2507 tests do not show reality, when they were tested with the Gleeble and their microstructural analyses were done, the result was not as desired. As we can see in figure 28, the microstructure of one of the samples does not seem to have undergone a heat treatment, presenting a fine banded microstructure, which differs from the desired microstructure as found in figure 33.

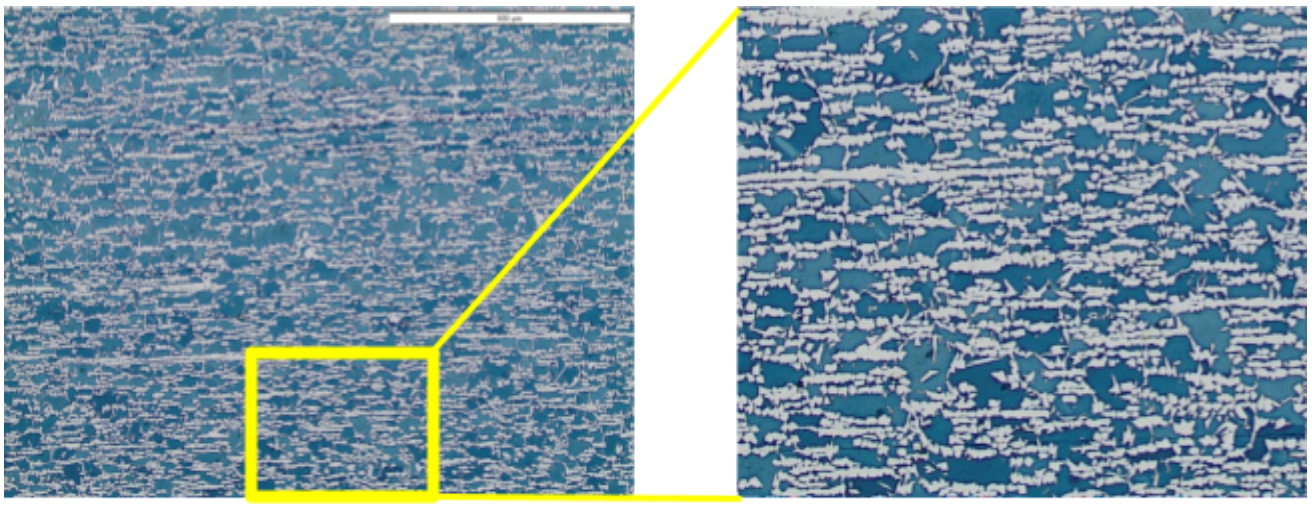

Figure 33 : Microstructure of a DX2507 that appears not to have undergone heat treatment at a sufficiently high temperature.

Aperam has already performed DX2507 tests successfully before, but with a different composition from the tests carried out during this project, and they worked, using a maximum programmed temperature of 1350°C.

When we compare DX2507 tested previously and DX2507 tested in this project, we don't find much difference in temperature, they are in the same range of values. So, we can say that the difference found in thermo-calc temperature A5 of +- 6°C, may in fact exist, as shown in figure 34.

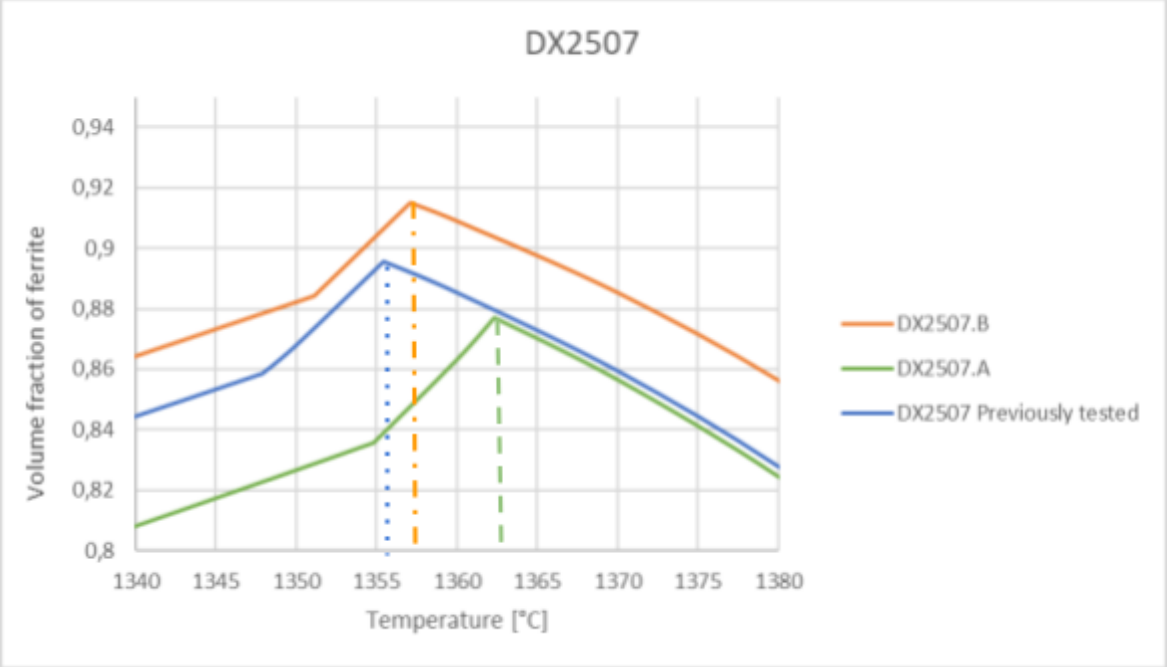

Figure 34 : Microstructure of a DX2507 that appears not to have undergone heat treatment

So, it brings us some questions to be worked on in the future by Aperam: does the thermo-calc in fact bring values close to real values? Is thermo-calc really right and the temperature of A5 is higher, so should the maximum temperature of the Gleeble program be increased?

Another problem found during the Gleeble tests was that when the quenching system is activated, the test result suffers a variation, which hinders a little in the analysis of the results since this variation happens around 1300°C, which is one of the points to be analyzed, since it is where there is phase transformation. (figure 35)

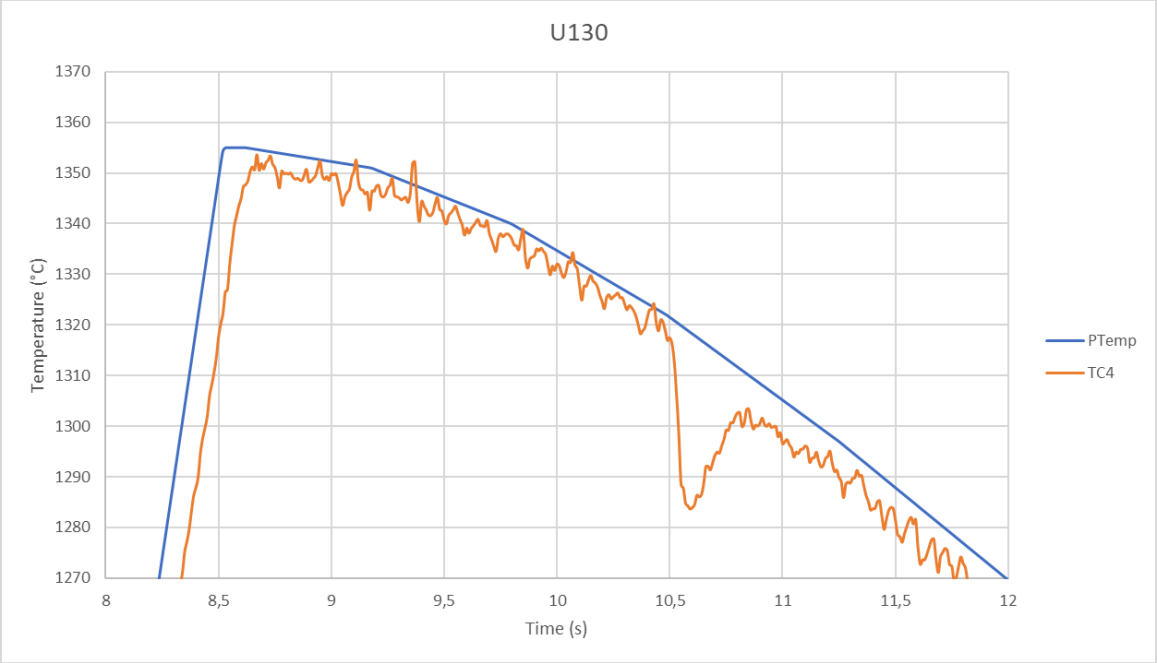

Figure 35 : Quenching system problem, variation at 1300°C

To adjust the problem found in figure 35, I tested changing the quenching system that was initially launched all at the same time, and changing to launch one first and another at a lower temperature. Another change to improve our curve and avoid this large variation was to lower the temperature at the beginning of the quenching, that initially it was around 1320-1300°C and then it started to be released around 1100-1200°C.

As can be seen in figure 36, the variation problems have decreased, making it possible to perform the analysis at 1300°C, to calculate the cooling rate and phase change analysis.

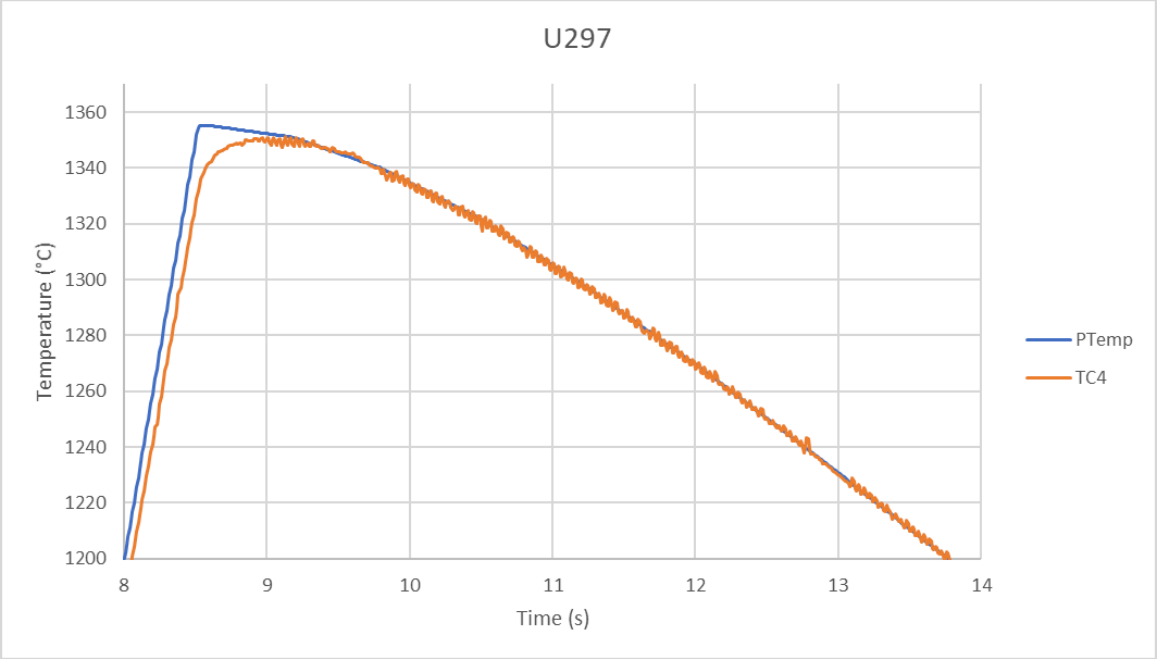

Figure 36 : Tempering system problem solved

Conclusion

During this internship, significant progress was made in understanding and optimizing the ferrite content in duplex stainless steels, particularly within the heat-affected zone (HAZ) during welding. The thermo-Calc proved to be an effective and important tool for thermodynamic simulations, enabling the prediction of duplex stainless steels' behavior during the welding process.

Although the simulations gives a close approximation of important parameters, it is known that the thermo-calc results are not the same as the measured values, as seen during the project with the microstructural analysis, however, after some tests we can imagine that perhaps the Thermo-Calc results are in fact close to the real values, articularly with the DX2507 grade. This shows that some conditions need to be changed in order to achieve higher accuracy.

The Gleeble 3800 machine was used to analyze and simulate welding conditions and of the effects of thermal cycles on the ferrite content, in a less expensive and faster way. The use of this machine helps to optimize the composition and welding processes, which was validated by a strong correlation found in the comparison between the experimental results with the microstructural analysis and the data produced by Thermo-Calc. However, some issues, such as the unexpected behavior of DX2507 and minor variations in cooling rates, indicate that further adjustments are needed to enhance accuracy and reliability.

Finally, after the results are found, some points of the project need to be improved. Such as: For the base formula for multiple duplex grades, it can be concluded that some elements did not have a linear behavior on the tested range, so it would therefore be necessary to test the quadratic terms and the interaction terms. Additionally, reconsidering conditions to work with the DX2507, maybe changing the maximum temperature of the Gleeble program could provide more accurate results.

Personally, working at Aperam has given me new knowledge, especially in metallurgy and more specifically in stainless steel duplex. It was my first experience in this field, and I had the chance to discover thanks to my year at Aperam and I liked it a lot. The opportunity to work at Aperam, utilizing advanced simulation tools and testing machines, has significantly expanded my practical skills and understanding in this field, providing a strong foundation for my future career in materials engineering.

Appendix

- ➔ Appendix 1: Aperam Company Organizational Chart
- ➔ Appendix 2: ThermoCalc 2024a with Database: TCFE9 Steels/ Fe-Alloys 9.3
- ➔ Appendix 3: Linearity of the first method thermo-calc
- ➔ Appendix 4: Each DSS family with the % variation of each elements
- ➔ Appendix 5: Python code
- ➔ Appendix 6: Buehler Samplmet Cutter
- ➔ Appendix 7: Secotom Precision Cutting Machine
- ➔ Appendix 8: Struers LaboForce-100
- ➔ Appendix 9: Results of thermodynamic simulation program Thermo-calc
- ➔ Appendix 10: Graphs of ferrite percentage versus tr8-5 (10 and 20s) and percentage versus cooling rate at 1300°C

Appendix 1: Aperam Company Organizational Chart

aperam

Aperam's Value Chain

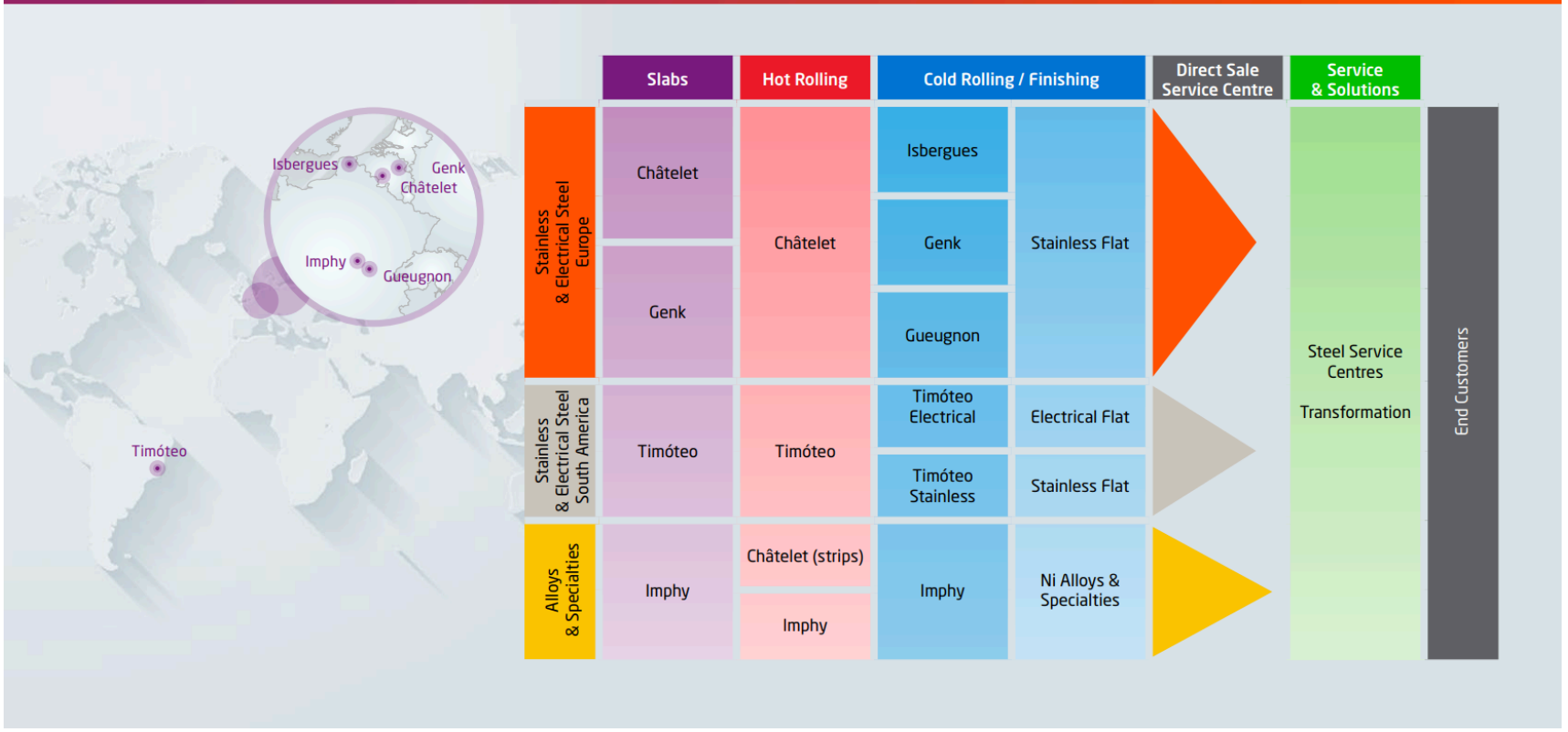

Appendix 2: ThermoCalc 2024a with Database: TCFE9 Steels/ Fe-Alloys 9.3

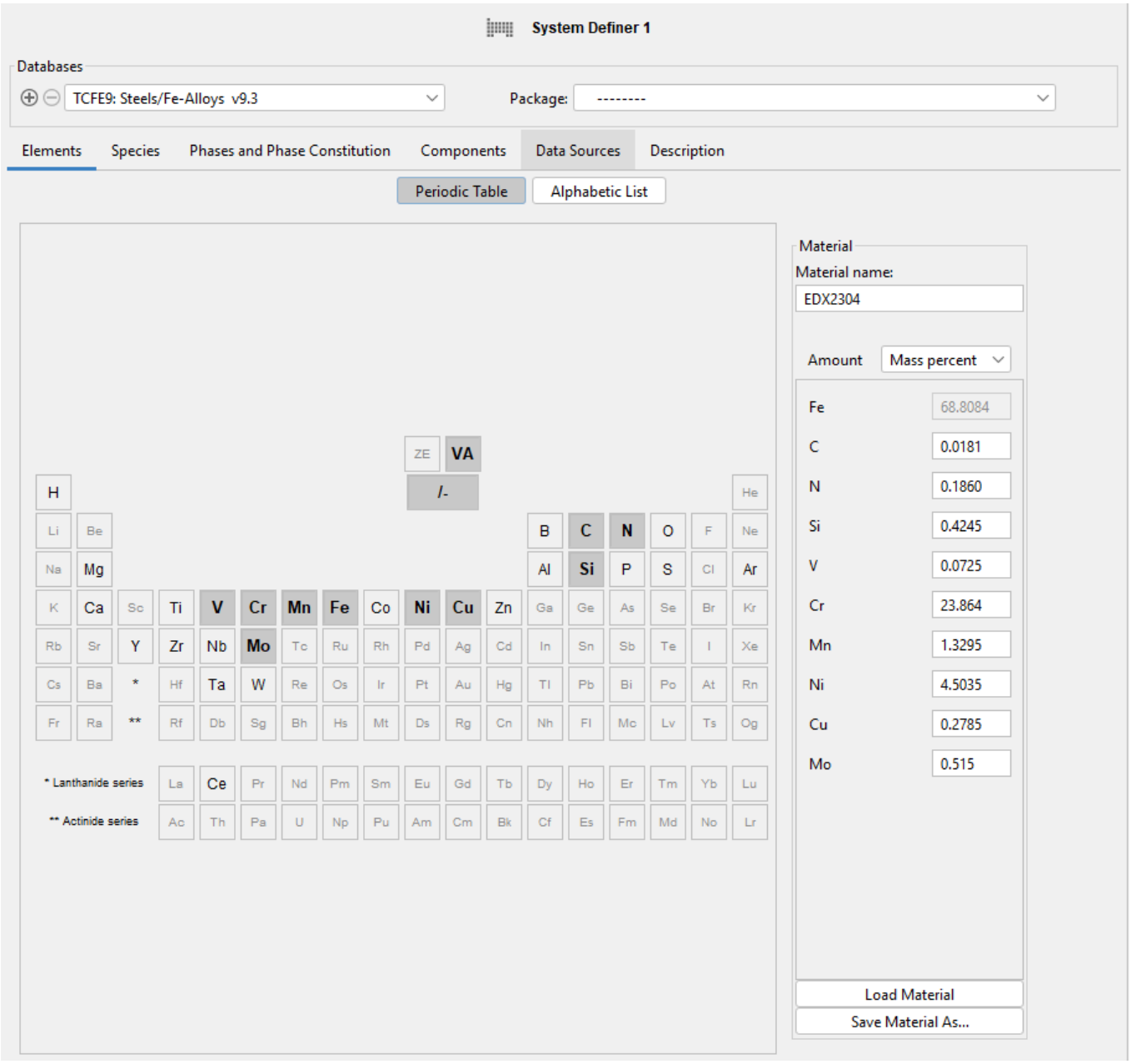

Appendix 3: The R^2 of the regression in method 1 to judge linearity

Cr2N	C	N	Si	V	Cr	Mn	Ni	Cu	Mo
AF21E3 - 00709535	1	0,9991	1	0,999	0,9969	0,9999	0,9993	1	1
AF21E5 - 024006330	1	0,9987	1	0,9992	0,997	0,9999	0,9995	1	1
AF23E3 - 25005333	1	0,9983	1	0,9993	0,9974	0,9994	0,9999	1	1
AF24E1 - 30705647	1	0,9985	1	0,9992	0,9967	0,9994	0,9999	1	1
AF46 - 91307739	1	0,9986	1	0,9993	0,9972	0,9999	0,9994	1	0,9999
AF47 - 52008467	1	0,9987	1	0,9992	0,9972	0,9999	0,9995	1	0,9999
AF61E3 - 94610543	1	0,9984	1	0,9996	0,9949	1	0,9994	1	0,9998

A5	C	N	Si	V	Cr	Mn	Ni	Cu	Mo
AF21E3 - 00709535	1	0,9999	1	1	1	0,9995	1	0,9998	1
AF21E5 - 024006330	1	0,9997	1	1	1	0,9989	1	0,9983	1
AF23E3 - 25005333	1	0,9996	1	1	1	0,9999	1	0,9994	1
AF24E1 - 30705647	1	0,9996	1	1	1	0,9109	1	1	1
AF46 - 91307739	1	0,9895	1	1	0,9998	0,999	1	0,993	0,9995
AF47 - 52008467	1	0,9969	1	1	1	0,9993	1	0,99	0,9997
AF61E3 - 94610543	1	0,9991	0,9999	1	0,9999	1	0,9991	1	0,9999

% ferrite 1200°C	C	N	Si	V	Cr	Mn	Ni	Cu	Mo
AF21E3 - 00709535	1	0,9999	0,9999	1	0,9979	0,9998	1	1	1
AF21E5 - 024006330	1	0,9999	0,9999	1	0,9979	0,9998	1	1	1
AF23E3 - 25005333	1	0,9999	0,9999	1	0,9965	0,9998	1	0,9999	1
AF24E1 - 30705647	1	0,9999	0,9998	1	0,997	0,9994	1	1	1
AF46 - 91307739	1	0,9999	1	1	0,9984	0,9998	1	1	0,9992
AF47 - 52008467	1	0,9999	0,9999	1	0,9984	0,9998	1	1	0,9994
AF61E3 - 94610543	1	0,9999	1	1	0,9986	0,9999	1	1	0,9993

Appendix 4: Each DSS family with the % variation of each elements

delta compo (% de %)		10	10	10	20	5	10	5	20	20			
éléments	Fe	C	N	Si	V	Cr	Mn	Ni	Cu	Mo	Composition unit	Temperature	Temperature unit
AF21E3	69,1138	0,0161	0,1001	0,41	0,12	23,18	1,47	4,82	0,32	0,45	mass_pct	1200	C
AF21E5	68,6071	0,0135	0,1594	0,4400	0,1100	23,6500	1,5500	4,4800	0,3800	0,6100	mass_pct	1200	C
AF23E3	71,2466	0,0197	0,1837	0,4600	0,1000	22,9300	1,9400	2,5800	0,2800	0,2600	mass_pct	1200	C
AF24E1	69,5551	0,0217	0,2202	0,7700	0,0730	21,7200	5,3600	1,6600	0,2300	0,3900	mass_pct	1200	C
AF46	66,1450	0,0190	0,1560	0,2300	0,1200	22,8000	1,7800	5,4700	0,2400	3,0400	mass_pct	1200	C
AF47	67,6856	0,0191	0,1653	0,4400	0,0900	22,0600	1,7700	5,0000	0,2500	2,5200	mass_pct	1200	C
AF61E3	61,9975	0,0158	0,2657	0,3900	0,0910	25,7100	0,8200	6,6600	0,3200	3,7300	mass_pct	1200	C

Appendix 5: Python code

```
import pandas as pd
import matplotlib.pyplot as plt

# Étape 1: Lire les données à partir du fichier Excel
caminho_arquivo = r"O:\APPRENTIS\JULIA NOLDIN\gleeble\2024.03.15 - 2024 - 03 HAZ\U374 - 250724a.d02.xlsx"
donnees = pd.read_excel(caminho_arquivo)

# Étape 2: Lisser la courbe de température (TC4)
donnees['TC4_lisse'] = donnees['TC4'].rolling(window=5).mean()

# Étape 3: Tracer la courbe de température en fonction du temps
plt.plot(donnees['Time'], donnees['TC4_lisse'], label='Température (TC4)')
plt.xlabel('Temps (s)')
```

```
plt.ylabel('Température (°C)')
plt.title('Courbe de température lissée')
plt.legend()
plt.grid(True)
plt.show()

# Étape 4: Calculer la température maximale réelle
temperature_maximale_reelle = donnees['TC4_lisse'].max()
print("Température maximale (TC4) :", temperature_maximale_reelle, "°C")

# Étape 5: Filtrer les données pour inclure uniquement les températures entre 200°C et 1200°C et avant d'atteindre la température maximale
donnees_filtrees_avant_max = donnees[(donnees['TC4_lisse'] >= 200) & (donnees['TC4_lisse'] <= 1200) & (donnees['Time'] <= donnees[donnees['TC4_lisse'] == temperature_maximale_reelle]['Time'].iloc[0])]

# Étape 6: Calculer la variation de température par rapport au temps pour déterminer la vitesse en °C/s
delta_temperature_avant_max = donnees_filtrees_avant_max['TC4_lisse'].iloc[-1] - donnees_filtrees_avant_max['TC4_lisse'].iloc[0]
delta_temps_avant_max = donnees_filtrees_avant_max['Time'].iloc[-1] - donnees_filtrees_avant_max['Time'].iloc[0]
vitesse_avant_max = delta_temperature_avant_max / delta_temps_avant_max
print("Vitesse de chauffage en °C/s entre 200°C et 1200°C (valeurs avant d'atteindre la température maximale) :", vitesse_avant_max, "°C/s")

# Étape 7: Filtrer les données pour inclure uniquement les températures entre 500°C et 800°C après avoir atteint la température maximale
indice_temperature_maximale = donnees[donnees['TC4_lisse'] == temperature_maximale_reelle].index[0]
donnees_temp_800_500 = donnees[(donnees['TC4_lisse'] >= 500) & (donnees['TC4_lisse'] <= 800) & (donnees.index > indice_temperature_maximale)]
```

```
# Étape 8: Trouver le moment où la température atteint la valeur la plus proche de 800°C
donnees_temp_800 = donnees_temp_800_500.loc[donnees_temp_800_500['TC4_lisse'].sub(800).abs().idxmin(), 'Time']

# Étape 9: Trouver le moment où la température atteint la valeur la plus proche de 500°C
donnees_temp_500 = donnees_temp_800_500.loc[donnees_temp_800_500['TC4_lisse'].sub(500).abs().idxmin(), 'Time']

# Étape 10: Calculer le temps en secondes entre les températures les plus proches
temps_entre_800_et_500 = abs(donnees_temp_500 - donnees_temp_800)
print("Temps en secondes entre les températures les plus proches de 800°C et 500°C après avoir atteint la température maximale:", temps_entre_800_et_500, "s")

# Étape 11: Filtrer les données pour inclure uniquement les températures entre 1275°C et 1325°C après avoir atteint la température maximale
donnees_filtrees_apres_max = donnees[(donnees['TC4_lisse'] >= 1275) & (donnees['TC4_lisse'] <= 1325) & (donnees['Time'] > donnees[donnees['TC4_lisse'] == temperature_maximale_reelle]['Time'].iloc[0])]

# Étape 12: Calculer la variation de température par rapport au temps pour déterminer la vitesse en °C/s
delta_temperature_apres_max = abs(donnees_filtrees_apres_max['TC4_lisse'].iloc[-1] - donnees_filtrees_apres_max['TC4_lisse'].iloc[0])
delta_temps_apres_max = donnees_filtrees_apres_max['Time'].iloc[-1] - donnees_filtrees_apres_max['Time'].iloc[0]
vitesse_apres_max = delta_temperature_apres_max / delta_temps_apres_max
print("Vitesse en °C/s entre 1275°C et 1325°C (après avoir atteint la température maximale) :", vitesse_apres_max, "°C/s")

# Étape 13: Filtrer les données pour inclure uniquement les températures supérieures à 1000°C
donnees_sup_1000 = donnees[donnees['TC4_lisse'] > 1000]

# Étape 14: Calculer le temps total pendant lequel la température est supérieure à 1000°C
```

```
temps_total_sup_1000 = donnees_sup_1000['Time'].iloc[-1] - donnees_sup_1000['Time'].iloc[0]
print("Temps total pendant lequel la température est supérieure à 1000°C:", temps_total_sup_1000, "secondes")

# Étape 15: Filtrer les données pour inclure uniquement les températures supérieures à 1100°C
donnees_sup_1100 = donnees[donnees['TC4_lisse'] > 1100]

# Étape 16: Calculer le temps total pendant lequel la température est supérieure à 1100°C
temps_total_sup_1100 = donnees_sup_1100['Time'].iloc[-1] - donnees_sup_1100['Time'].iloc[0]
print("Temps total pendant lequel la température est supérieure à 1100°C:", temps_total_sup_1100, "secondes")

# Étape 17: Filtrer les données pour inclure uniquement les températures supérieures à 1200°C
donnees_sup_1200 = donnees[donnees['TC4_lisse'] > 1200]

# Étape 18: Calculer le temps total pendant lequel la température est supérieure à 1200°C
temps_total_sup_1200 = donnees_sup_1200['Time'].iloc[-1] - donnees_sup_1200['Time'].iloc[0]
print("Temps total pendant lequel la température est supérieure à 1200°C:", temps_total_sup_1200, "secondes")

# Étape 19: Identificar os índices onde a temperatura atinge o valor máximo
indices_temp_max = donnees[donnees['PTemp'] == donnees['PTemp'].max()].index

# Étape 20: Calcular a diferença de tempo entre o primeiro e o último índice onde a temperatura é máxima
if len(indices_temp_max) > 1:
    temps_entre_temp_max = donnees.loc[indices_temp_max[-1], 'Time'] - donnees.loc[indices_temp_max[0], 'Time']
else:
    temps_entre_temp_max = 0

# Étape 21: Imprimir o tempo total em que a temperatura permanece no máximo
print("Temps total où la température reste au maximum (PTemp):", temps_entre_temp_max, "secondes")
```

Appendix 6: Buehler Samplmet Cutter

Appendix 7: Secotom Precision Cutting Machine

Appendix 8: Struers LaboForce-100

Appendix 9: Results of thermodynamic simulation program Thermo-calc

Grade	Coil number	T(°C) point A5	% ferrite à 1200°C	T(°C) Cr2N
DX1803	520XXXXX	1363,4	66%	1079,9
DX2101	307XXXXX	1341,7	72%	1091,7
DX2202	128XXXXX	1335,2	77%	1131,7
DX2202	215XXXXX	1351,0	72%	1122,8
DX2202	241XXXX0	1345,4	74%	1117,0
DX2202	241XXXX4	1342,0	76%	1122,8
DX2202	218XXXXX	1334,9	76%	1145,5
DX2202	250XXXXX	1325,5	77%	1109,3
DX2205	144XXXXX	1368,0	68%	1119,3
DX2205	210XXXXX	1368,0	67%	1110,3
DX2205	913XXXXX	1358,8	70%	1089,7
DX2304	007XXXXX	1307,2	75%	1031,6
DX2304	119XXXXX	1320,1	73%	1045,9
DX2304	420XXXXX	1289,8	80%	1032,1
DX2304	043XXXXX	1311,1	76%	1008,8
DX2304	441XXXXX	1303,2	78%	1042,0
DX2304+	024XXXXX	1338,6	71%	1090,1
DX2304+	529XXXXX	1316,2	77%	1113,2
DX2507	201XXXXX	1362,4	58%	1115,9
DX2507	421XXXXX	1355,5	62%	1164,1
DX2507	640XXXXX	1358,7	60%	1155,5
DX2507	122XXXXX	1356,4	65%	1135,2
DX2507	946XXXXX	1357,1	64%	1165,5

Appendix 10: Graphs of ferrite percentage versus tr8-5 (10 and 20s) and percentage versus cooling rate at 1300°C

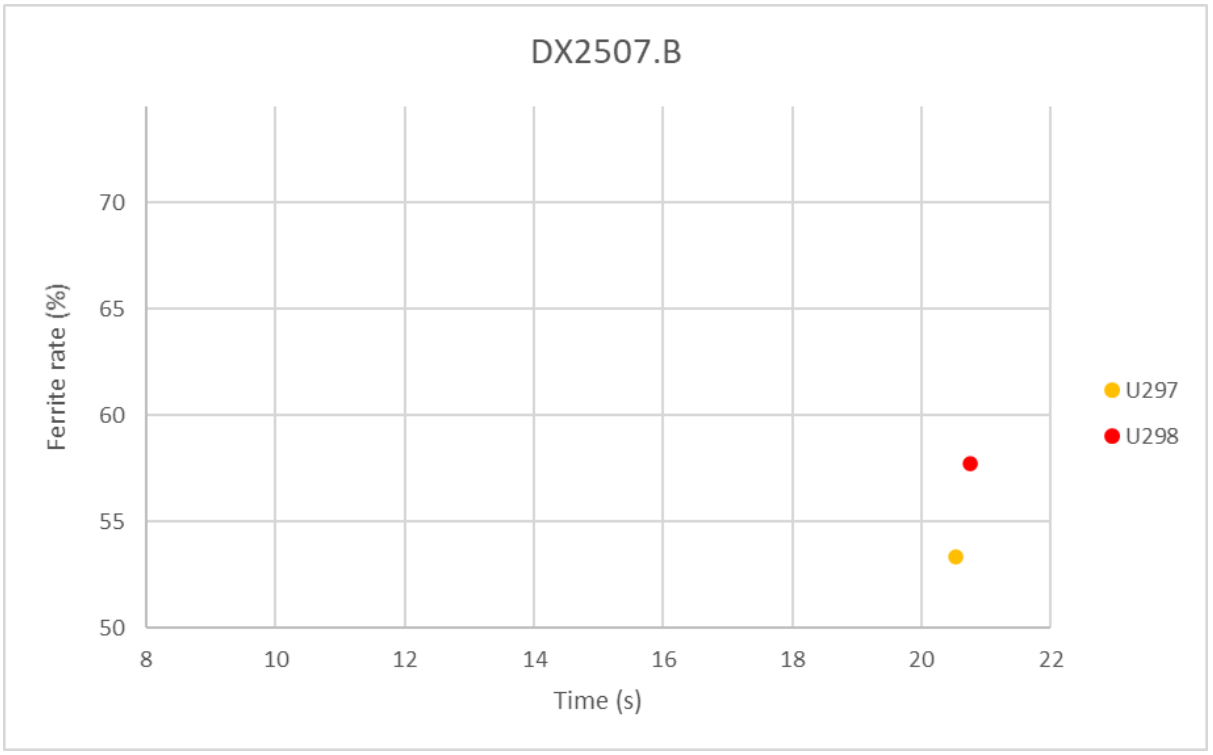

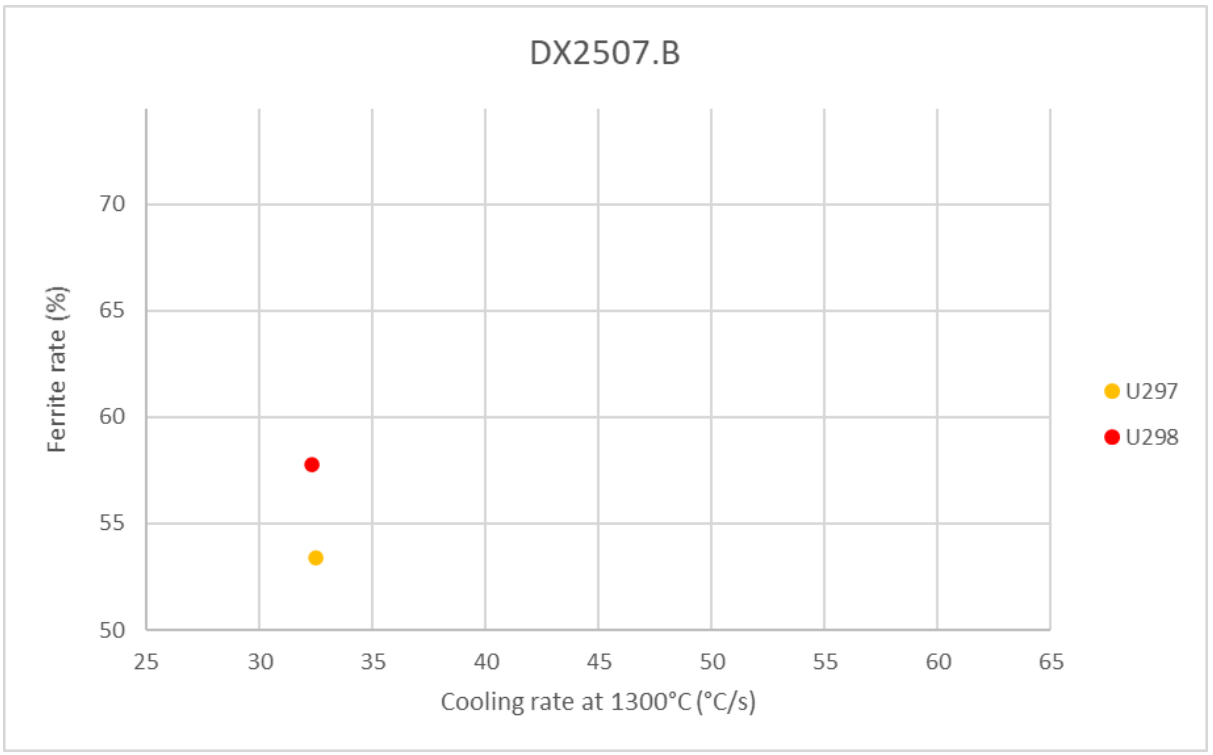

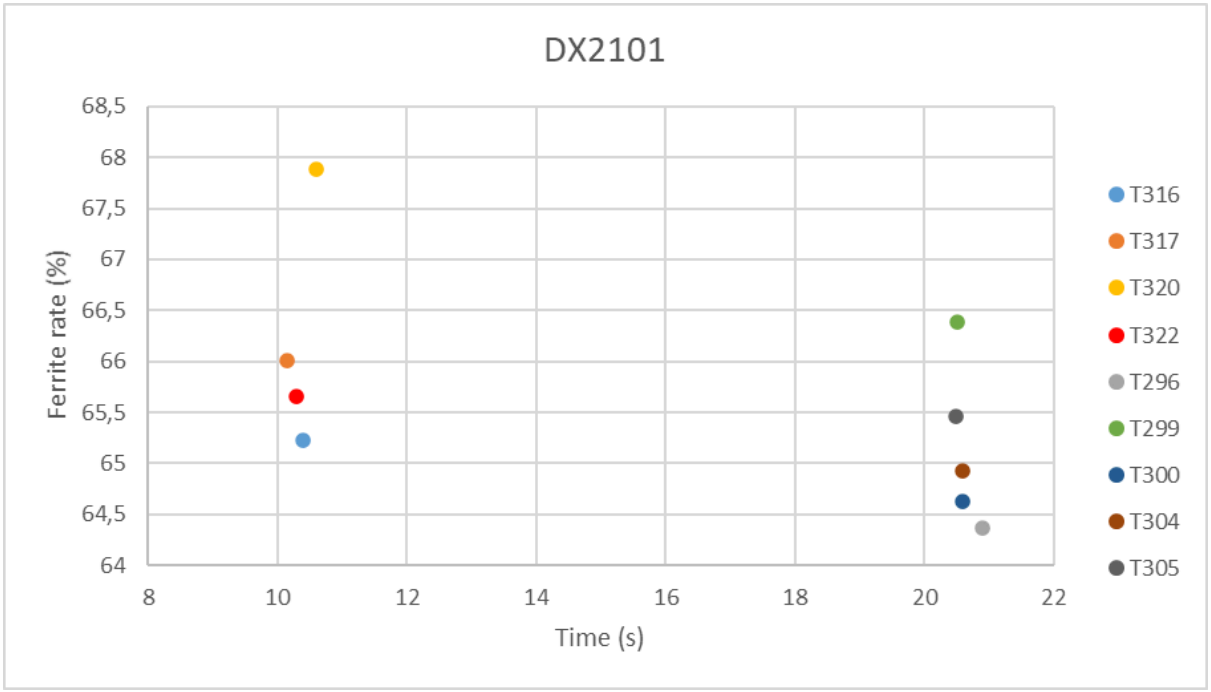
DX2101
Ferrite rate (%)
68,5
68
67,5
67
66,5
66
65,5
65
64,5
64
8
10
12
14
16
18
20
22
Time (s)
T316
T317
T320
T322
T296
T299
T300
T304
T305

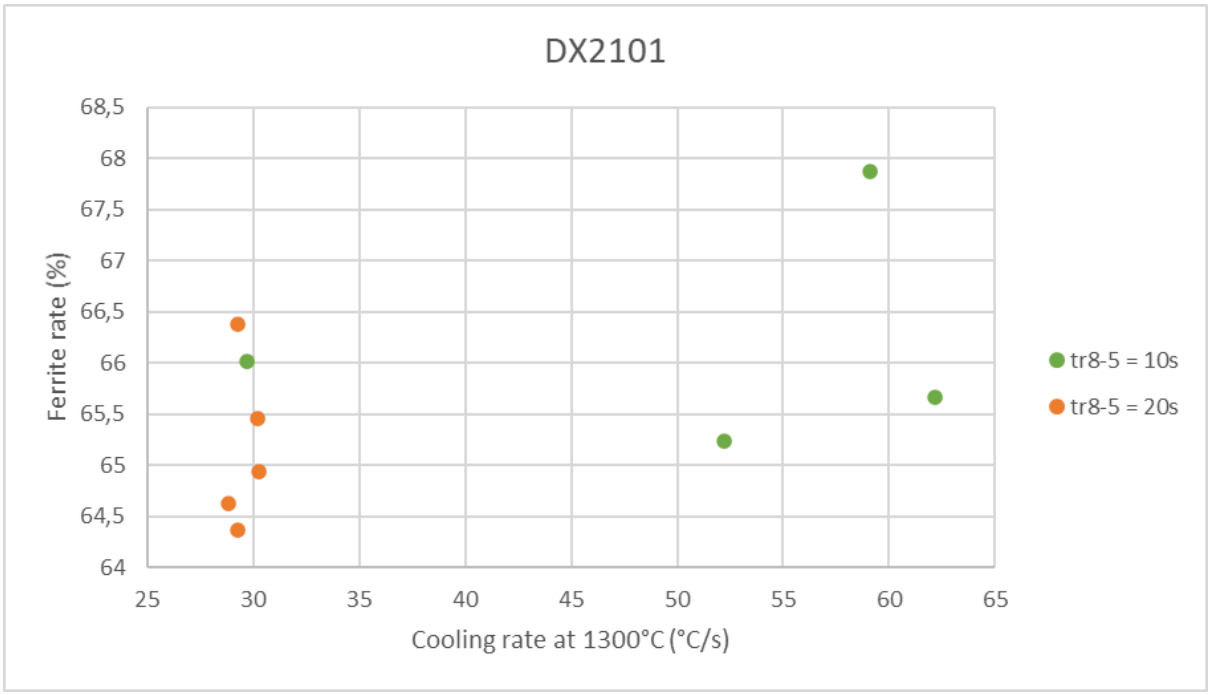
DX2101
Ferrite rate (%)
68,5
68
67,5
67
66,5
66
65,5
65
64,5
64
25
30
35
40
45
50
55
60
65
Cooling rate at 1300°C (°C/s)
tr8-5 = 10s
tr8-5 = 20s

Bibliographie

1. Home - aperam. (2024, 13 mai). Aperam. https://www.aperam.com/
2. ISSF. (s. d.). Basic facts about stainless steel. Dans worldstainless.org. Consulté le 6 mai 2024, à l'adresse https://www.worldstainless.org/media/ka3dwqnk/basic-facts-about-stainless-steel.pdf
3. Maslak, M.; Stankiewicz, M.; Slazak, B. Duplex Steels. Encyclopedia. Available online: https://encyclopedia.pub/entry/16149 (accessed on 12 August 2024).
4. Welding Metallurgy and Weldability of Stainless Steels, by John C. Lippold and Damian J. Kotecki. 06/05/2024
5. Alvarez-Armas, Iris, and Degallaix-Moreuil, Suzanne, eds. Duplex stainless steels. John Wiley & Sons, 2013.
6. V.S. Moura, L.D. Lima, J.M. Pardal, A.Y. Kina, R.R.A. Corte, S.S.M. Tavares, Influence of microstructure on the corrosion resistance of the duplex stainless steel UNS S31803,Materials Characterization, Volume 59, Issue 8
7. A Hosseini, Vahid. (2016). Influence of multiple welding cycles on microstructure and corrosion resistance of a super duplex stainless steel.
8. Zucato, Igor & C, Moreira & Machado, Izabel & Lebrão, Susana. (2002). Microstructural Characterization and the Effect of Phase Transformations on Toughness of the UNS S31803 Duplex Stainless Steel Aged Treated at 850 °C. Materials Research. 5. 10.1590/S1516-14392002000300026.
9. Iacoviello, Francesco & Di Cocco, Vittorio & Franzese, E & Natali, Stefano. (2008). Fatigue crack propagation micromechanisms in high temperature embrittled duplex stainless steels. 17th European Conference on Fracture

2008: Multilevel Approach to Fracture of Materials, Components and Structures. 3.

10. Comment réaliser le soudage des aciers austéno-ferritiques duplex et superduplex ? (s. d.). https://www.soudeurs.com/site/comment-realiser-le-soudage-des-aciers-austeno-ferritiques-duplex-et-superduplex-280/

11. Candel EHP. Soldagem dos aços inoxidáveis superduplex UNS S32750 e UNS S32760 [dissertação]. São Paulo: Universidade de São Paulo; 2016.

12. Borges, Ferdinando & Borges, Wenio & Santos, Rafaela & Leal, Valdemar & Dos Santos Júnior, José & Lobo, Anderson & Sousa, Rômulo. (2021). Corrosion Resistance and Microstructural Evaluation of a Plasma Nitrided Weld Joint of UNS S32750 Super Duplex Stainless Steel. Materials Research. 24. 10.1590/1980-5373-mr-2021-0087.

13. Computational Materials Engineering - Thermo-Calc software. (2024, 25 juillet). Thermo-Calc Software. https://thermocalc.com/

14. Quigley, D. (2024, août 26). MS&T - October 6–9, 2024 - Pittsburgh, Pennsylvania, USA. Dynamic Systems For Materials Research. https://gleeble.com/products/gleeble-systems/gleeble-3800.html

15. D. ROSENTHAL, the theory of moving sources of heat and its application to metal treatments, transaction of the ASME, 1946.